Master's thesis
Theoretical Physics

Dimensional reduction in the study of the electroweak phase transition

Lauri Niemi

April 4, 2018

UNIVERSITY OF HELSINKI
DEPARTMENT OF PHYSICS

PL 64 (Gustaf Hällströmin katu 2)
00014 University of Helsinki

HELSINGIN YLIOPISTO — HELSINGFORS UNIVERSITET — UNIVERSITY OF HELSINKI

Tiivistelmä — Referat — Abstract

First-order phase transitions in the electroweak sector are an active subject of research as they contain ingredients for baryon number violation and gravitational-wave production. The electroweak phase transition in the Standard Model (SM) is of a crossover type, but first-order transitions are possible in scalar extensions of the SM, provided that interactions of the Higgs boson with the new particles are sufficiently strong. If such particles exist, they are expected to have observable signatures in future collider experiments. Conversely, studying the electroweak transition in theories beyond the SM can bring new insight on the cosmological implications of these models.

Reliable estimates of the properties of the transition require non-perturbative approaches to quantum field theory due to infrared problems plaguing perturbative calculations at high temperatures. We discuss three-dimensional effective theories that are suitable for lattice simulations of the transition. These theories are constructed perturbatively by factorizing correlation functions so that contributions from light field modes driving the phase transition can be identified. Resummation of infrared divergences is naturally carried out in the construction procedure, and simulating the resulting effective theory on the lattice allows for a non-perturbative phase-transition study that is also free of infrared problems. Dimensionally-reduced theories can thus be used to probe the conditions under which perturbative treatments of the electroweak phase transition are valid.

We apply the method to the SM augmented with a real SU(2) triplet scalar and provide a detailed description of dimensional reduction of this model. Regions of a first-order transition in the parameter space are identified in the heavy triplet limit by the use of an effective theory for which lattice results are known. We provide a rough estimate for the accuracy of our results by considering higher-order operators that have been omitted from the effective theory and discuss future prospects for the three-dimensional approach.

Contents

1 Introduction

Explaining the observed asymmetry in the numbers of baryons and their antiparticle counterparts is a long-standing problem in particle physics and cosmology. Most recent cosmological observations suggest a baryon to entropy density ratio of [1]

$$\frac{\rho_B}{s} = (8.61 \pm 0.09) \times 10^{-11}, \tag{1.1}$$

and while the behavior of antimatter is described well by quantum field theories (QFT), the origin of this baryonic excess remains a mystery. Furthermore, if this asymmetry was something the universe was born with, any excess of particles of either kind is expected to be quickly washed away by thermal fluctuations in the early universe [2]. This suggests that the universe was initially matter-antimatter symmetric with a vanishing total baryon number B. The symmetry is then broken at some later stage by an unknown baryogenesis process.

Minimum requirements for baryogenesis to occur are summarized in the three Sakharov's conditions [3]:

1. Existence of baryon number violating processes

2. Violation of both C and CP symmetries

3. Interactions outside of thermal equilibrium.

While the first requisite is self-explanatory, the remaining conditions are necessary to prevent baryon number compensation by antimatter-producing processes. Various mechanisms satisfying all three Sakharov's conditions have been proposed, many of which rely on physics beyond the Standard Model (SM) of particle physics (see Refs. [4–6] for reviews). The baryonic excess should be produced before light elements are formed in the primordial nucleosynthesis [7], and most proposed models predict baryogenesis at energy scales ranging from that of Grand Unification Theories (GUT) to the electroweak (EW) scale.

One particularly interesting scenario is electroweak baryogenesis (EWBG), which attempts to explain generation of the observed baryon number during the spontaneous symmetry breaking of the $\mathrm{SU}(2)_L \times \mathrm{U}(1)_Y$ gauge symmetry and takes place in a hot plasma of interacting particles in the early universe [6, 8–15]. In the language of thermodynamics, the transition corresponds to a Bose-condensation of the Higgs field [16–19] and occurs at a critical temperature of $T_c \sim 100$ GeV [17, 18]. The two phases are characterized by the vacuum expectation value (vev) v of the Higgs field. The third Sakharov's condition requires this transition to be of first-order, so that thermodynamic quantities of relevance change discontinuously as the universe transitions into the present EW vacuum of $v = 246$ GeV in the minimal SM. Such transitions proceed by bubble nucleation, in which expanding bubbles of the broken phase form inside the symmetric phase. This nucleation is a consequence of metastability of the $v = 0$ vacuum state at temperatures higher than T_c. During the transition, the two phases are separated by bubble walls of finite thickness, and as the bubbles expand, particles in the plasma are forced to interact with the walls.

These interactions provide a framework in which all Sakharov's conditions are satisfied and a baryonic excess can be generated.

Baryon number B violation in the SM manifests itself via the axial anomaly [20]. The processes responsible for B violation are topologically non-trivial field configurations satisfying the classical equations of motion. These correspond to transitions from one degenerate $SU(2)_L$ minimum to another, and for baryogenesis, the most interesting solutions are sphalerons, corresponding to classically passing over the potential barrier separating two minima [21]. Sphalerons are strongly amplified by the external temperature, and at the electroweak scale of $T \sim 100$ GeV, sphaleron transition rates become unsuppressed and are able to cause significant baryon number violation [22–24].

However, the sphalerons are CP-symmetric, and external CP violation is thus needed to produce a net baryon asymmetry. This is achieved via scattering processes in the vicinity of the bubble walls: the SM provides CP violation via a complex phase in the Cabicco-Kobayashi-Maskawa (CKM) matrix, causing fermions and antifermions to have different transition amplitudes when interacting with the bubble boundaries [25, 26]. The magnitude of this CP violation determines the total amount of baryons created during the transition. Finally, for any baryonic excess produced in the electroweak phase transition (EWPT) to survive, the sphaleron rate has to become suppressed after the transition ends. In the phase of broken $SU(2)_L$ symmetry, sphalerons are suppressed by a Boltzmann factor whose magnitude is directly related to the strength of the transition, characterized by the latent heat [23, 27]. The minimum criterion for a successful EWBG is therefore a strong first-order phase transition, accompanied by a suitable amount of CP violation.

Independently of the question of baryogenesis, a first-order EWPT may also act as a source of gravitational waves [28, 29]. These are produced as the bubbles of broken phase expand and interact with the surrounding plasma, causing friction and converting vacuum energy into kinetic energy. Strong enough phase transitions are expected to leave behind gravitational-wave signatures that could be observed in the near future with detectors such as LISA [30].

Making quantitative estimates of the final baryon number density or the gravitational-wave power spectrum requires comprehensive knowledge of bubble nucleation dynamics in the plasma, such as the speed at which the bubbles expand [10]. Computation of many of these quantities in perturbation theory is unreliable due to the non-equilibrium nature of the transition and infrared (IR) problems related to perturbative expansions in the symmetric phase [10, 31, 32]. Non-perturbative methods are thus needed for quantitative studies of the EWBG and possible gravitational-wave signals.

The most robust non-perturbative results are obtained by directly simulating the system on a lattice. Lattice simulations, however, suffer from slow convergence due to the sign problem when applied to theories containing chiral fermions, such as the SM [33]. One way to bypass this problem is provided by the effective theory approach in which fermionic fields can be integrated out, resulting in a simpler theory that can be studied on the lattice. In practice, the effective theory is most conveniently constructed by using dimensional reduction (DR), a well-defined technique for building three-dimensional (3d) effective field theories from the full four-dimensional (4d) theory at high temperature

[34, 35]. The method is based on factorization of fields into static and time-dependent components, the latter of which generate effective masses via their interactions with the surrounding plasma. Static long-distance Green's functions of the full theory can then be reproduced to a good accuracy by a time-independent 3d theory containing only the static field modes. DR produces a direct temperature-dependent mapping from the 4d fields and couplings to parameters of the 3d theory. In particular, the effective theory contains no fermions, whose effects have been encoded into the coupling constants and fields of the dimensionally-reduced theory. Furthermore, the 3d theory is super-renormalizable, providing a great simplification for lattice analyses.

Extensive lattice simulations performed on a dimensionally-reduced effective theory in the 1990's have demonstrated that the EWPT in the SM is inadequate for baryogenesis [36, 37]. In particular, the measured Higgs boson mass $m_H = 125$ GeV results in an analytic crossover instead of a first-order transition [35, 38], rendering EWBG impossible in the SM. Similar results have been obtained from simulations in the full 4d theory with a discarded fermion sector in Refs. [39, 40]. Furthermore, even if the transition was of first order, the CP violation provided by the CKM matrix would be insufficient to produce the observed baryonic excess [41–43]. Remarkably, perturbative approaches using the effective potential in the full 4d theory tend to overestimate both the order and the strength of the transition, at least in the SM case [44].

Modern research of EWBG is centered around extensions of the SM and their effects on the EWPT. New particles in the Higgs sector can considerably modify dynamics of the transition and may allow for extra CP violation beyond that of the CKM matrix, as well as provide strong first-order phase transitions. An essential feature of these extended models is that for EWBG to be possible, the new scalar fields cannot be much more massive than the electroweak scale and must couple to the Higgs doublet with moderate strength [14]. These properties imply that the predictions of EWBG models should be testable in collider experiments in the near future. This property is the main advantage of EWBG over its strongest competitor, leptogenesis, which assumes new physics only at an energy scale of 10^{10} GeV [45–47].

Despite the IR catastrophe of high-temperature QFT, which causes a breakdown of perturbative expansions when massless particles are present [10, 31, 32], the primary method of EWPT studies in Beyond Standard Model (BSM) theories today is to use the perturbative effective potential. While these analyses are generally easy to perform relative to a full lattice study, the reliability of the fully perturbative approach is questionable already on theoretical grounds. In addition to the IR problems, it has been known for a long time that the traditional effective potential approach is inadequate for calculation of gauge invariant quantities relevant for baryogenesis [48, 49]. An alternative perturbative method for constructing the effective potential in a gauge-invariant way has been discussed in Refs. [50, 51], but this method is particularly sensitive to higher-order loop corrections. On the other hand, gauge fixing on the lattice is not required at all, and the parameter mappings produced by DR can be explicitly shown to be gauge invariant [35].

Recently, attempts to validiate perturbative results by analyzing the nature of the EWPT using dimensionally-reduced effective theories have arisen in various BSM models.

One of these is the triplet Higgs extension, in which the SM is augmented with an SU(2) triplet scalar field Σ. This model has been studied perturbatively in the context of the EWPT in Ref. [52] and, more recently, non-perturbatively using DR in Ref. [53], on which this thesis is based on. DR has also been used to study the EWPT in the Minimally Supersymmetric Standard Model in [54–56], the Two Higgs Doublet Model in [57–60] and the real singlet extension of the SM in [61].

The aim of this thesis is to present a detailed description of the dimensionally-reduced effective theory approach to studying the EWPT non-perturbatively. We begin reviewing the mathematical formalism needed to describe field theories at nonzero temperatures in section 2.1, before proceeding to discuss the framework of dimensional reduction in section 3. For the latter part of the thesis we focus on the triplet Higgs model, describing its general properties and dimensional reduction of the model in detail in sections 4 and 5. Finally, in section 6 we use existing lattice results to find regions of a first-order phase transition in the limit of a heavy triplet field. The results presented here have previously been published in the main paper [53], while many omitted technical and computational details are presented in this thesis. In particular, a diagrammatic calculation of the correlation functions needed to construct the DR mappings are presented in the appendices.

2 Aspects of thermal field theory

As a prerequisite for understanding dimensional reduction, we start by reviewing how statistical mechanics is incorporated into QFT. Since thermal field theory by itself is a vast area of theoretical physics, we shall only concentrate on topics of importance for DR. Throughout the thesis we shall use a natural system of units by setting $c = k_B = \hbar = 1$.

2.1 Imaginary time formalism

In statistical mechanics, the main quantity of interest is the partition function Z, defined in terms of the Hamiltonian H as

$$Z = \operatorname{Tr} e^{-\beta H} = \sum_\phi \langle \phi | e^{-\beta H} | \phi \rangle \tag{2.1}$$

with β being the inverse temperature. Thermodynamic quantities, such as free energies, can be calculated from Z by direct differentation, and we would now like to construct a field theoretical counterpart of the partition function. The most practical way of achieving this is to let the time coordinate take on imaginary values. In this section, we shall mainly describe the formalism for the case of a scalar field theory for simplicity, as more complicated systems are treated in a similar manner.

Consider the path integral representation for the amplitude that a field configuration changes from $|\phi_0\rangle$ at time $t = 0$ to $|\phi'\rangle$ at some later time $t = t'$. The path integral can be expressed in Hamiltonian formalism by performing a Legendre transformation on the Lagrangian, $\mathcal{L} = \pi\dot{\phi} - \mathcal{H}(\phi, \pi)$, and integrating over the conjugate momentum π:

$$\langle \phi' | e^{-iHt} | \phi_0 \rangle = N \int D\pi \, D\phi \, \exp\left[i \int_0^{t'} dt \int d^3x \big[\pi\dot{\phi} - \mathcal{H}(\phi, \pi) \big] \right]. \tag{2.2}$$

Here N is a normalization factor. Next, consider Wick rotating the system to Euclidean spacetime by analytically continuing the time variable onto the imaginary axis, $\tau = it$. If the Hamiltonian density is at most quadratic in π, we can bring the rotated path integral back to the Lagrangian form by completing the square and performing the momentum integral. For a careful analysis of how this is done in a more general case, where e.g. gauge fields are present, see Refs. [62, 63]. The result after integrating over the canonical momentum is a functional integral resembling the usual path integral of quantum field theory,

$$\langle \phi' | e^{-H\tau} | \phi_0 \rangle = N' \int D\phi \, \exp\left[\int_0^{\tau'} d\tau \int d^3x \, \mathcal{L}(\tau = it, \phi, \dot{\phi}) \right]. \tag{2.3}$$

The form of the new normalization factor N' is irrelevant, as it cancels when calculating correlation functions.

It is now clear that by requiring that the field returns to its initial value after time τ' and identifying the period as the inverse temperature $\beta = 1/T$, one gets a path integral expression for the partition function in Euclidean space. However, integration is now

restricted to only include paths that are periodic in the imaginary time coordinate. The partition function has then the schematic form

$$Z[\phi] = \int D\phi \, e^{-S_E}, \tag{2.4}$$

where we have defined the Euclidean action as

$$S_E = \int_0^{1/T} d\tau \int d^3x \, \mathcal{L}_E, \tag{2.5}$$

and the Euclidean Lagrangian is obtained from its Minkowskian counterpart by $\mathcal{L}_E = -\mathcal{L}_M(\tau = it)$. From now on, we will drop the subscripts and work solely in the Euclidean formalism, unless stated otherwise.

The equilibrium dynamics of the theory are characterized by Euclidean correlation functions, which can be computed from the path integral using familiar methods from zero-temperature QFT, with the modification that the metric is now Euclidean. Note, however, that we explicitly break rotational symmetry by imposing periodicity on the time coordinate but not on the spatial coordinates. Physically, this can be interpreted to mean that a system coupled to a heat bath has a preferred frame of reference, and therefore Lorentz invariance does not hold in finite temperature QFT [62, 63].

The periodicity of the field ϕ implies that one can represent it as a Fourier series expansion in the imaginary time coordinate τ. We therefore write

$$\phi(\tau, \mathbf{x}) = \sum_{n=-\infty}^{\infty} \tilde{\phi}(\omega_n, \mathbf{x}) e^{i\omega_n \tau}. \tag{2.6}$$

From the above discussion it follows instantly that for scalar fields and, in fact, for bosonic fields in general, $\omega_n^b = 2\pi n T$. For fermionic fields, there is a complication arising from their anti-commutative nature, and Fourier modes for fermions are characterized by $\omega_n^f = (2n+1)\pi T$ [62, 63]. These frequences are called *Matsubara modes* and the case of bosonic $n = 0$ is called the *Matsubara zero-mode*. In particular, bosonic fields have a vanishing zero-mode, while fermions do not. Remarkably, the bosonic $n = 0$ modes are static in the sense that the exponential containing dependence on the temporal coordinate τ vanishes.

A Fourier expansion with respect to the remaining spatial coordinates is readily constructed by restricting the system into a finite volume V and taking the limit $V \to \infty$. The temporal coordinate remains discrete and has to be treated carefully when performing momentum-space loop calculations. A *Matsubara sum-integral* is associated with each loop momentum (in $D = 4 - 2\epsilon$ dimensions):

$$T \sum_n \int \frac{d^d p}{(2\pi)^d}, \tag{2.7}$$

where $d = D - 1$. We adopt the shorthand notation

$$T \sum_n \int_p \equiv \sumint_P, \tag{2.8}$$

which is understood to include the integration measure as well as any constant factors associated with it.

Computation of these thermal sum-integrals is usually done by applying techniques from complex analysis after a careful change of integration and summation order. It is worth noting that one can always separate the Matsubara zero-mode from other modes in the sum and write

$$\sum\!\!\!\!\!\!\int_P = T \int_{p,n=0} + \; \sum\!\!\!\!\!\!\int_P'{}^{,} \tag{2.9}$$

where all non-zero modes are included in the primed sum-integral. This separation is useful in construction of dimensionally-reduced theories where it is important to distinguish between static and time-dependent field modes.

2.2   Effective masses and the thermal scale hierarchy

An important consequence of thermal field theory is that fields generate temperature-dependent effective masses. For concreteness, let us first see how this occurs for a scalar field of mass m_0. As discussed in the previous section, periodicity in the imaginary time coordinate has the consequence that the temporal momentum component becomes discretized, $P = (\omega_n, \mathbf{p})$. The free Euclidean propagator in momentum space is found by Wick-rotating the Klein-Gordon operator and reads

$$\tilde{G}_0(P) = \frac{1}{P^2 + m_0^2} = \frac{1}{\mathbf{p}^2 + \omega_n^2 + m_0^2}. \tag{2.10}$$

This corresponds to the propagator of a field mode of mass $\sqrt{\omega_n^2 + m_0^2}$. Using perturbation theory, one is able to calculate loop corrections to the mass of the original scalar field. This correction obtains contributions from all Matsubara modes via sum-integrals, and the one-loop corrected mass has the form $m(T)^2 = m_0^2 + \gamma T^2$, where γ depends on the type of the field in question and m_0 is the zero-temperature mass. The temperature-dependent term is understood as an effective thermal mass and its existence reflects the fact that the propagation of the field is altered by its interactions with the heat bath.

Consider now a Yang-Mills theory possessing gauge invariance. In zero-temperature QFT, gauge fields are generally made massless by their corresponding Ward identities. The situation becomes more complicated when considering systems at finite temperatures as the heat bath breaks Lorentz invariance, forcing the temporal component of a vector gauge field to behave differently from its spatial counterparts. Physically, this behaviour arises from the fact that presence of mobile charge carriers causes exponential damping in the corresponding interaction strength. This phenomenon is known as *screening* and occurs in both electroweak theory and quantum chromodynamics (QCD) [62, 63]. For our purposes, the relevant heat bath is a hot plasma in the early universe with temperature $T \sim 100$ GeV. Damping caused by the plasma manifests itself as a T-dependent effective mass, called the Debye mass m_D, in the temporal gauge field component when loop corrections are taken into account. The spatial components, on the other hand, are protected by gauge invariance and remain massless.

In the SM, there are three gauge fields C_μ, A_μ, B_μ, associated with the $\mathrm{SU}(3)_c$, $\mathrm{SU}(2)_L$ and $\mathrm{U}(1)_Y$ symmetries respectively, that all generate effective masses. Their Debye masses can be computed perturbatively by calculating the gauge field two-point functions to the required loop order and identifying the arising correction to the propagator [63]. In section 3.3, we compute them as a natural part of dimensional reduction, but at this stage, it is useful to note that the Debye mass of a gauge field is proportional to the respective gauge coupling. In particular, the $n = 0$ mode of the temporal $\mathrm{SU}(2)$ gauge field A_0 has the thermal mass $m_D \sim gT$.

Let us now consider the situation from the point of view of the Matsubara field modes. We may interpret each of these modes as an independent field, with their respective mass parameters having the form $m_n^2 = m_0^2 + \omega_n^2$, meaning that all bosonic $n \neq 0$ modes obtain a mass correction of order πT. The Matsubara frequencies for fermions are $\omega_n^f = (2\pi n + 1)T$, implying that the thermal mass correction for all fermionic modes is always of $O(\pi T)$. We now observe that the heat bath has generated a natural scale hierarchy in the system: At sufficiently large temperatures, thermal corrections to the masses of the Matsubara modes will dominate over the zero-temperature masses, so that the bosonic modes with $n \neq 0$ and all fermionic modes have effective masses of order πT, while the zero-mode of A_μ has mass proportional to gT. The canonical terminology here is to call the thermal scale πT *superheavy* and the scale gT *heavy*. In addition, the scale g^2T – which can arise if the loop correction to a mass parameter is close to cancelling the tree-level mass – is dubbed *light*. Spatial gauge fields that remain completely massless are also included in this category.

In a realistic model describing the EWPT, there should exist a scalar field that spontaneously breaks the electroweak symmetry. In the SM, this role is played by the Higgs field ϕ, with its potential being $V(\phi) = -\mu_\phi^2(\phi^\dagger\phi) + \lambda(\phi^\dagger\phi)^2$. The transition occurs when the initial minimum of the potential at $\phi = 0$ becomes a metastable state due to a decrease in the temperature, and in the tree-level potential, this corresponds to a change of sign in the squared mass. At the critical temperature, the mass parameter is thus forced to be light due to a cancellation caused by the thermal mass correction.

The emergence of a thermal scale hierarchy suggests the possibility of constructing simplified effective theories for describing physics at different energy scales. For large T, the superheavy scale becomes so massive that its effect on long-distance physics is negligible. Integrating the superheavy fields out from the partition function results in a theory for heavy and light fields that is considerably easier to use for studying the EWPT than the full theory. Similar reasoning can be applied to the scale gT to integrate out the heavy scale as well; this gives a theory containing only light field modes. These considerations underlay the discussion of section 3, where we give a detailed description of the effective theory approach.

2.3   The infrared problem of perturbative calculations

Perturbative calculations of quantum correlators in the imaginary time formalism come with intrinsic problems related to small momenta [31, 32]. The situation is especially grief in the symmetric phase, where all known fields, with the exception of the Higgs doublet, are massless. Formally, these IR divergences arise from the leading contributions of

bosonic propagators inside loop integrals, i.e, from Matsubara zero-modes. The appropriate expansion parameter for high-T perturbative expansions is $\rho \sim g^2 n_B(E)$, where

$$n_B(E) = \frac{1}{e^{-E/T} - 1} \tag{2.11}$$

is the Bose distribution function, arising from the thermal loop integrals, and E corresponds to the energy of individual particles in the plasma [62, 63].

The distribution function obtains its largest contribution from the Matsubara $n = 0$ modes, and in particular, the largest expansion parameter for bosonic fields is $\rho \sim g^2 T/m$, indicating a breakdown of perturbation theory in the limit $m \to 0$. Conversely, all fermionic and $n \neq 0$ bosonic propagators contain an effective thermal mass and are IR safe, even if the fields in vacuum were massless. Perturbation theory for the superheavy scale, constructed using the expansion parameter $\rho \sim g^2/T^2$, is then free of IR problems and valid for large T. In the broken phase, an IR cutoff is provided by the gauge boson masses and the SU(2) sector can thus be treated perturbatively. However, knowledge of the system in the symmetric phase is indispensable for quantitative analysis of the EWPT, and the IR problems have to be accounted for when performing perturbative calculations.

The breakdown of perturbative expansions can be postponed by identifying the IR-divergent contributions and summing them together to infinite order in perturbation theory [64, 65]. This is known as *thermal resummation* and has the effect of generating a dynamical mass that dampens IR divergences in the problematic propagators. However, this method of IR regularization can become cumbersome at higher loop orders, and resummation of the light scale is especially problematic as the loop-corrected masses can be close to zero. For these reasons, it is often more convenient to implement resummation via an effective theory approach. We shall discuss resummation in detail in the context of dimensional reduction in section 5.4.

3 Dimensional reduction

The emergence of a thermal mass hierarchy suggests that at length scales parametrically larger than $1/gT$, both superheavy and heavy fields decouple from physics. The statement of dimensional reduction is that there exists a mapping from the full 4d theory at high temperature to a simpler Euclidean theory in three dimensions that only contains light fields and procudes the same long-distance Green's functions as the underlying theory. Originally applied to QCD to study its high-T behavior [66, 67], it was realized in the 1990's that the same method of DR could be used to facilitate lattice studies of the EWPT [34, 35]. The resulting effective theory possesses 3d gauge invariance and is able to describe physics of the EWPT at sufficient accuracy via the remaining scalar zero-modes. In practice, construction of this mapping requires perturbative computation of several two- and four-point functions. In this section, we describe how the dimensionally-reduced theory can be constructed by an explicit matching of Green's functions and discuss the conceptual foundations of the method.

3.1 High-temperature effective theories

To illustrate the basic principles behind dimensional reduction, consider a general renormalizable gauge field theory in a 4d Euclidean space and write the fields in terms of their Fourier components as in Eq. (2.6). When the expansions are inserted into the path integral, the partition function factorizes into integrals over zero-modes and modes with $\omega_n \neq 0$. The Matsubara zero-modes contain no dependence on the imaginary time, and the integration over τ can, in principle, be trivially carried out for the zero-modes. The remaining field modes obtain thermal masses of order $\sim \pi T$, and at a high temperature, decouple from physics at distances larger than $1/T$.

The bosonic $n = 0$ mode part of the action is then treated as an effective action for a time-independent theory, obtained by integrating out the decoupled superheavy modes. Before going into details about how this theory is, in practice, constructed, let us make a few historical remarks about effective theory approaches to thermal field theory. The original method of constructing high temperature dimensionally-reduced theories, described in [66], consists of writing an effective action of the form

$$e^{-S_{\text{eff}}} = \int D\psi D\phi_{n\neq 0} \, e^{-S} \tag{3.1}$$

and perfoming integrations over superheavy fields. The effective action is then to be calculated perturbatively to the desired order in $1/T$, dropping all induced higher-order operators. As has been pointed out in Refs. [35, 68], a perturbative computation of S_{eff} constructed from Eq. (3.1) is problematic due to the emergence of non-local operators caused by the integration over the superheavy fields. All diagrams integrated out in this way consist solely of superheavy internal lines, ignoring diagrams that can additionally contain light propagators. Since light fields interacting with superheavy fields can have momenta on the scale of T, the effect of these diagrams cannot be expanded in terms of p^2/T^2, causing a breakdown of perturbation theory when attempting to calculate S_{eff}.

While this complication has been taken into account in more modern approaches (see [69] for a review), we will follow the method introduced in Refs. [34, 35] that bypasses the problem discussed above by using an explicit matching of the static Green's functions of the full and effective theories. Super-renormalizability of the effective 3d theory plays an important role in construction of the parameter mapping and will be discussed in detail in section 5.3. It is useful to carry this matching procedure out in two separate steps, first mapping the full 4d theory to a 3d theory for heavy and light scales, and then integrating the remaining heavy fields out of the theory. It is worth emphasizing that in this method, fields are not actually "integrated out" in the Wilsonian sense as the effective theory is constructed simply by first writing down a field theory in three dimensions, and then defining its parameters so that the effective vertices match those of the underlying theory.

Throughout the thesis, we shall describe DR with the assumption that the underlying 4d theory is an SM-like gauge theory in the unbroken $SU(2)_L \times U(1)_Y$ phase, unless stated otherwise.

3.2   Construction of the heavy-scale theory by parameter matching

To facilitate the upcoming discussion, we adopt a power counting scheme similar to that of Ref. [35]. All relevant gauge and Yukawa couplings are assumed to scale as $\sim g$, where g is the $SU(2)$ coupling, while scalar couplings scale as $\sim g^2$. The main purpose of this power counting is to provide a systematic method for estimating the accuracy of dimensionally-reduced effective theories. In Ref. [35], the scaling assumption $g' \sim g^{3/2}$ was presumed for the $U(1)$ coupling; we choose to use the power counting $g' \sim g$ to obtain slightly more accurate matching relations. We shall perform DR perturbatively to $O(g^4)$ accuracy, with the exception of Debye mass computations, which we only do at $O(g^2)$ accuracy.

Consider a finite-temperature theory containing only static bosonic modes. This theory can possess 3d gauge invariance and contain gauge, ghost and scalar fields, which we identify as the Matsubara zero-modes of the fields of an underlying 4d theory. The Lagrangian bears no time dependence, and effectively corresponds to a 3d field theory. We can write the action as

$$S_{\text{eff}} = \frac{1}{T} \int d^3x \; \mathcal{L}_{3d}, \tag{3.2}$$

where the prefactor $1/T$ follows from the integral over τ. The 3d theory is super-renormalizable due to the reduced number of spacetime dimensions, providing a significant simplification over the full theory. In order for this theory to be a true effective theory for the underlying 4d theory, we define its parameters so that to a given accuracy, the connected Green's functions of this theory match to the static Green's functions of the full theory.

To see how this matching can be performed, consider the Higgs doublet in four dimensions, with the potential $V(\phi) = m^2 \phi^\dagger \phi + \lambda (\phi^\dagger \phi)^2$ and with the mass being either heavy or light. Suppose this theory has a 3d counterpart with the 3d fields ϕ_3 corresponding to the $n = 0$ modes of the 4d theory. The 3d scalar potential has the same form as in four dimensions, but the mass and the coupling are different, denoted m_3 and λ_3. In the 3d

theory, we can write the renormalized two-point function for the field ϕ_3 as

$$\tilde{G}_3^{-1}(p) = p^2 + m_3^2 - \Pi_3(p^2), \tag{3.3}$$

where $\mathbf{p}$ is an external 3d momentum and the self-energy $\Pi_3(p^2)$ contains loop corrections from one-particle-irreducible (1PI) diagrams evaluated in the 3d theory[1]. Since the 3d theory consists of heavy and light field modes only, $\Pi_3(p^2)$ receives no corrections from fields at the superheavy scale.

Next, consider the analogous quantity in the 4d theory, evaluated for the Matsubara zero-modes:

$$\tilde{G}^{-1}(P) = P^2 + m^2 - \Pi(P^2), \tag{3.4}$$

where $P = (0, \mathbf{p})$ is now the $n = 0$ external momentum in four Euclidean dimensions and the Π-function receives correction from superheavy field modes in addition to the heavy and light contributions. By requiring that the $n = 0$ mode corresponds to the scalar field ϕ_3 in the 3d theory, we can separate the self-energy into a contribution from zero-modes only that is reproduced by the 3d theory, and an additional contribution that comes solely from diagrams containing superheavy propagators. We write the self-energy as

$$\Pi(P^2) = \Pi_3(p^2) + \bar{\Pi}(p^2), \tag{3.5}$$

where superheavy diagrams are contained in $\bar{\Pi}(p^2)$. Strictly speaking, Π_3 is reproduced correctly only if resummation is implemented in the 4d theory. We shall postpone this discussion until section 5.4.

Analyticity of $\bar{\Pi}(p^2)$ is guaranteed by the fact that the superheavy scale is free of IR problems, so for $p \ll T$ it can be expanded in the external momentum p^2. Following our power counting scheme, already the p^4 term in the expansion will be of order $O(g^6)$ if the momentum is restricted to the heavy scale ($p \lesssim gT$). Thus

$$\bar{\Pi}(p^2) = \bar{\Pi}(0) + \bar{\Pi}'(0)p^2 + O(g^6), \tag{3.6}$$

where it is assumed that $\bar{\Pi}'(0)$ has been computed to $O(g^2)$ accuracy and $\bar{\Pi}(0)$ to $O(g^4)$ accuracy, corresponding to one-loop and two-loop orders respectively.

We can now write the 4d two-point function as

$$\tilde{G}^{-1}(P) = [1 - \bar{\Pi}'(0)] \left\{ p^2 + [m^2 - \bar{\Pi}(0)][1 + \bar{\Pi}'(0)] - \Pi_3(p^2) \right\}, \tag{3.7}$$

which is equivalent to Eq. (3.4) up to terms of order $O(g^4)$. It is then straightforward to match Eq. (3.7) against the two-point function in the effective theory, Eq. (3.3), by demanding that the fields are related as

$$(\phi^\dagger \phi)_{3d} = \frac{1}{T}[1 - \bar{\Pi}'(0)](\phi^\dagger \phi)_{4d} \tag{3.8}$$

---

[1]We find it convenient to define the self-energy with a minus sign. Π is then given directly by the sum of 1PI diagrams [62].

and that the mass in the 3d theory is given by

$$m_3^2 = [m^2 - \bar{\Pi}(0)][1 + \bar{\Pi}'(0)]. \tag{3.9}$$

Note that we have absorbed the factor of $1/T$ multiplying the action into the normalization of the 3d fields. The fields then have mass dimensionality of $1/2$. A one-loop computation of the correction to the field normalization suffices, as the product $m^2\bar{\Pi}'(0)$ is then of $O(g^4)$ when the 4d mass is heavy.

Other fields and couplings can be matched in a similar fashion, by calculating renormalized correlation functions to a given order in g and deriving matching relations as above. $O(g^4)$ accuracy for mass parameters generally requires perturbative computation of self-energy correlators to two-loop order, while for coupling constants, a one-loop calculation of their respective four-point correlators is sufficient. For example, the quartic coupling λ_3 in three dimensions can be matched by directly equating the effective vertices of the two theories:

$$-2\lambda_3 T(\delta_{ij}\delta_{jk} + \delta_{il}\delta_{jk})(\phi_i^\dagger\phi_j\phi_k^\dagger\phi_l)_{3\mathrm{d}} = [-2\lambda + \bar{\Pi}_4(0)](\delta_{ij}\delta_{jk} + \delta_{il}\delta_{jk})(\phi_i^\dagger\phi_j\phi_k^\dagger\phi_l), \tag{3.10}$$

where $\bar{\Pi}_4(0)$ is the renormalized one-loop correction from the superheavy modes to the four-point function, and the SU(2) structure has been written down explicitly. The coefficient T on the left-hand side follows from the definition of 3d fields. Taking into account the field normalization factor in Eq. (3.8), the 3d coupling is then given to $O(g^4)$ by

$$\lambda_3 = T\left(\lambda + 2\lambda\bar{\Pi}'(0) - \frac{1}{2}\bar{\Pi}_4(0)\right). \tag{3.11}$$

Note that for couplings appearing in more than one vertex, such as g, it is sufficient to calculate the correction to just one of the relevant vertices, and the final matching relations will not depend on this choice.

In some BSM theories, additional complications can arise due to reducible diagrams that are not necessarily reproduced by the effective theory. Such situation arises in, for example, models containing multiple Higgs doublets [54, 60]. If the second doublet is integrated out as a heavy field, the two-loop diagram depicted in Fig. 1 is not reproduced by the resulting 3d theory due to the internal heavy line connecting the two 1PI parts. This diagram has to be explicitly included in the matching procedure for the connected Green's functions to match.

Since the matching procedure is performed perturbatively, usual constraints of perturbation theory hold. In particular, DR becomes unreliable if the couplings of the full 4d theory are large. The accuracy of the resulting effective theory can be estimated by calculating higher-order correlation functions in the 4d theory and explicitly matching their effect to the heavy-scale theory. This allows for a simple power-counting estimate for the accuracy at which the static Green's functions are reproduced. If the heavy-scale parameters are matched at $O(g^4)$ accuracy, the theory is able to reproduce the light and heavy Green's functions up to terms of order g^4 [35]. We will discuss the omitted dimension-six operators further in section 5.6.
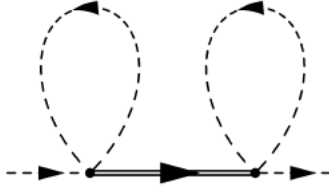
Figure 1: Example of a reducible diagram that needs to be included when performing matching. If the double line is a superheavy propagator, this diagram is not reproduced by the effective theory.

3.3   Induced adjoint scalars in the heavy-scale theory

As an illustrative example of the matching procedure, let us continue the discussion of section 2.2 about the temporal components of gauge fields. Dimensional reduction of vector fields requires extra care. We would like to write an effective 3d theory that incorporates effects of the temporal gauge field components, despite the fact that at most 3d gauge invariance is expected in this theory. Broken Lorentz symmetry in the temporal direction and the generation of a Debye mass suggest that the Matsubara zero modes of these temporal components should behave not as gauge fields, but as massive scalars in the effective theory.

Consider the Standard Model in the imaginary time formalism. Focusing especially on the SU(2) field A_μ and ignoring the other gauge fields for simplicity, we write a heavy-scale Lagrangian for a SU(2) *temporal scalar* adjoint field A_0 in three dimensions as follows:

$$\mathcal{L}_{\text{temporal}}^{(3)} = \frac{1}{2}(D_r A_0^a)_3^2 + \frac{1}{2}m_D^2(A_0^a A_0^a)_3 + h_3(\phi^\dagger \phi A_0^a A_0^a)_3 + \frac{1}{4}\kappa_3(A_0^a A_0^a)_3^2. \tag{3.12}$$

Here m_D is the Debye mass and the subscripts denote a 3d field or coupling. This is the most general 3d scalar Lagrangian consistent with SU(2) gauge symmetry, and our claim is that A_0 can be directly matched to the zero-component of A_μ in the full 4d theory.

Following the matching procedure described above, we need to calculate the two-point correlator of the temporal gauge field component A_0 in the 4d theory at external momentum P. To get a full $O(g^4)$ result, we would need the correlator at two-loop order. However, the effect of the temporal scalars on DR in total is small compared to that of the superheavy scale [35], so we shall be content with the much simpler one-loop result.

The self-energy correction has been calculated in Refs. [35, 61]. In order to counter inevitable ultraviolet (UV) divergences, dimensional regularization in $D = 4 - 2\epsilon$ dimensions has been used in conjunction with the $\overline{\text{MS}}$ renormalization scheme. The fully renormalized result in the SM reads

$$A_0^a \mathbin{\sim\!\!\!\bigcirc\!\!\!\sim} A_0^b = -g^2\delta_{ab}\left[T^2\frac{11}{6} - \frac{P^2}{16\pi^2}\left(1 + \frac{25}{6}L_b - 4L_f)\right)\right], \tag{3.13}$$

14

where $P = (0, \mathbf{p})$, and dependence on the renormalization scale Λ has been incorporated into the shorthand notations

$$L_b = 2 \ln \frac{\Lambda}{T} - 2[\ln(4\pi) - \gamma], \tag{3.14}$$

$$L_f = L_b + 4 \ln 2, \tag{3.15}$$

with γ being the Euler-Mascheroni constant.

According to Eq. (3.8), we then find that the corresponding field $(A_0^a)_3$ in the 3d theory is given by

$$(A_0^a A_0^a)_{3d} = \frac{(A_0^a A_0^a)_{4d}}{T} \left[1 - \frac{g^2}{16\pi^2} \left(1 + \frac{25}{6} L_b - 4 L_f \right) \right]. \tag{3.16}$$

The Debye mass can then be calculated from Eq. (3.9), with the 4d mass parameter being zero. Note, however, that by restricting ourselves to $O(g^2)$ calculation of m_D, the derivative term can be neglected, as its contribution is of $O(g^4)$. The result is thus

$$m_D^2 = g^2 T^2 \frac{11}{6}, \tag{3.17}$$

showing explicitly that $m_D \sim gT$. Therefore, the temporal scalar $(A_0^a)_3$ is indeed a heavy field, justifying its inclusion in the 3d theory.

3.4   Effective theory for the light scale

The effective 3d theory constructed above can be further simplified by integrating out the heavy degrees of freedom. These include the temporal scalar fields and possible additional heavy scalars that do not directly take part in the phase transition. The resulting theory is a 3d theory containing only light field modes and is valid for momenta $p \leq g^2 T$. It can be constructed by performing parameter matching similarly as in the case of the heavy-scale theory. For example, two-point function of a light scalar field is

$$\tilde{G}_3^{-1}(p) = p^2 + m_3^2 - \Pi_3(p^2) - \bar{\Pi}_3(p^2), \tag{3.18}$$

where $\bar{\Pi}_3(p^2)$ receives contributions from heavy fields and can be expanded in the external momentum p. We may now write down the corresponding two-point function in the light-scale theory,

$$\tilde{G}_{3,\text{light}}^{-1}(p) = p^2 + \bar{m}_3^2 - \Pi_3(p^2), \tag{3.19}$$

and follow the recipe given in section 3.2. This results in the matching relations

$$(\phi_3^\dagger \phi_3)_{\text{light}} = [1 - \bar{\Pi}'(0)](\phi_3^\dagger \phi_3), \tag{3.20}$$

$$\bar{m}_3^2 = [m_3^2 - \bar{\Pi}(0)][1 + \bar{\Pi}'(0)]. \tag{3.21}$$

Couplings are, again, matched by comparing the effective vertices. Loop corrections should be computed to $O(g_3^4)$ for consistency; the leading order matching results are then of $O(g^4)$. In practice, this step of DR is often simpler to perform than the first step due to the lack of superheavy field modes, as well as because of the super-renormalizable nature of the 3d theories. We may again estimate the validity of this DR step by computing omitted higher-order operators. Green's functions computed in the light-scale theory are within $O(g^3)$ of the respective 4d Green's functions (see section 5.6).

3.5   Phase transitions in the light-scale theory

Of particular interest is the light-scale theory obtained by performing DR on the SM. After the first step of DR, the only remaining heavy fields are the temporal scalars A_0, B_0 and C_0. Integrating them out leaves a theory containing only the 3d gauge fields and a light scalar field that drives a phase transition in the effective theory. To be precise, this theory is only valid near the transition, as the scalar field cannot be guaranteed to be light otherwise. The scalar potential is

$$V(\phi) = \bar{\mu}_3(\phi^\dagger \phi) + \bar{\lambda}_3(\phi^\dagger \phi)^2, \tag{3.22}$$

where the fields and couplings are now understood to be those of the light scale theory. Since this simpler theory is constructed to reproduce the same long distance physics as the underlying 4d theory, it can be used to study various properties of the EWPT. In particular, non-perturbative lattice simulations are more readily performed on the light-scale theory than the full 4d theory due to the lack of fermions. However, we emphasize that the utility of DR is limited to studying time-independent quantities, since the effective theories are completely static with respect to the temporal coordinate.

In the context of non-perturbative EWPT studies, a good approximation to the SM is given by a $SU(2)+$ Higgs theory, as the effect of the $U(1)$ field on the transition is small [37]. Notably, the dimensionally-reduced form of this theory only contains three parameters that the transition can depend on: the gauge coupling $\bar{g}_3$, the scalar mass $\bar{\mu}_3$ and the quartic coupling $\bar{\lambda}_3$. After dimensional reduction, the full light scale Lagrangian reads

$$\mathcal{L}_{\text{light}} = \frac{1}{4} F^a_{rs} F^a_{rs} + (D_r \phi)^\dagger (D_r \phi) + \bar{\mu}_3(\phi^\dagger \phi) + \bar{\lambda}_3(\phi^\dagger \phi)^2, \tag{3.23}$$

where $D_r \phi = (\partial_r - i\bar{g}\frac{\sigma}{2} \cdot \mathbf{A}_r)\phi$ is a spatial covariant derivative and F_{rs} is the $SU(2)$ field strength tensor. Note that we have suppressed irrelevant ghost and gauge-fixing terms.

Due to the matching procedure used to construct the theory, the parameters $\bar{g}_3, \bar{\mu}_3, \bar{\lambda}_3$ are dimensionful and have intrinsic temperature-dependence. It is convenient to parametrize the theory using the dimensionless quantities

$$x \equiv \frac{\bar{\lambda}_3}{\bar{g}_3^2}, \quad y \equiv \frac{\bar{\mu}_3^2}{\bar{g}_3^4}. \tag{3.24}$$

At tree-level, transition from the symmetric to the broken phase occurs when the squared mass parameter changes sign. The mass obtains temperature dependence from the matching procedure and in general, has the form

$$\bar{\mu}_3^2 = m^2 + \Gamma(T), \tag{3.25}$$

with m being the mass in the underlying full theory. $\Gamma(T)$ is the thermal correction obtained by integrating out superheavy and heavy fields. The tree-level transition occurs when the 4d mass is cancelled by the thermal effects encoded in $\Gamma(T)$, causing the minimum to shift from its original location at $\phi = 0$ to a non-zero field value. The actual critical line is not exactly at $y = 0$ due to radiative corrections [37], but we shall approximate the

critical point to be that at which the y parameter changes sign. It is then possible to find the critical temperature by varying the temperature inputted into the matching relations. However, in order to obtain additional information about the transition, such as the latent heat or the nucleation rate, further analysis using either perturbative or lattice methods is required.

The theory defined in Eq. (3.23) has been studied non-perturbatively on the lattice in Ref. [36], where it was found that the transition is of first order if $0 < x \lesssim 0.11$ at the critical temperature, while for $x \gtrsim 0.11$, the transition is of a crossover type, meaning that all derivatives of thermodynamic quantities are continuous. Furthermore, the transition becomes increasingly stronger the closer x is to zero. If $x < 0$, the potential is no longer bounded from below and the effective theory breaks down. This can happen if the perturbative construction of the matching relations has failed, in particular, when the omitted higher-dimension operators are large enough to cause considerable errors (see section 5.6).

DR accompanied with the above lattice results was applied to the Standard Model in Ref. [35]. A remarkable finding is that in the SM, the electroweak phase transition is of first order only if the Higgs mass has an unphysically small value of $m_H \lesssim 75$ GeV, and is a crossover for larger m_H. The endpoint at which the transition turns into a crossover is not achievable perturbatively [44], highlighting the importance of lattice approaches. We also stress that the DR procedure is free of the IR problems that usually plague high-T perturbation theory. This is because the IR divergences are caused by massless propagators of Matsubara zero-modes, but we have only performed integrations over superheavy and heavy field modes, which are IR finite. The problematic zero-modes can then be treated completely non-perturbatively on the lattice. There is one complication arising at two-loop level where diagrams can contain mixed $n = 0$ and $n \neq 0$ propagators, and resummation needs to be applied. The resummations are, however, easy to implement for $O(g^4)$ DR, and the perturbative expansions remain IR finite (for details, see section 5.4).

We emphasize that the light-scale theory in Eq. (3.23), and the existing lattice results for it, are also useful in the study of the EWPT in scalar extensions of the SM. If the additional scalar fields appearing in the theory are sufficiently heavy, corresponding to masses of order $\sim gT$ or larger, it is possible to integrate them out in either the first or the second step of DR. This results in a light-scale theory identical to the one discussed in this section – neglecting the U(1) field – with modified matching relations, and a non-perturbative analysis can be carried out without the need for new simulations. Note, however, that dynamical information is lost when fields are integrated out, and the effective theory of Eq. (3.23) is unable to describe phase transitions in which more than one light scalar take part in the symmetry breaking.

Finally, we point out that it is also possible to apply perturbative methods to the 3d theories. The downside of this approach is that by construction, the effective theories possess the same IR behavior as the underlying theory, and an effective potential constructed from the effective theory will thus suffer from the same IR problems as a similar approach in four dimensions. However, since proper resummations for the heavy and superheavy scales have been implemented when constructing the effective theories, we can expect better convergence near the phase transition than what is achieved in the full theory [70]. A

3d perturbative analysis may therefore be useful for improving the results obtained from the corresponding 4d effective potential. This has been performed for the SM in Ref. [34].

4 The triplet Higgs model

For the rest of this thesis, we shall concentrate on the triplet extension of the SM, abbreviated ΣSM. It is a model where, in addition to the usual Higgs doublet, a real-valued scalar field Σ belonging to the adjoint representation of the SU(2) group is introduced. New particle content in the ΣSM includes a neutral scalar Σ^0 and a charged scalar pair $\Sigma^\pm$. What makes the triplet model particularly interesting in the study of baryogenesis is its ability to produce a phase transition occuring in two steps [52]. The first step consists of isospin symmetry breaking for the triplet field, while in the second step, there is a transition from the isospin breaking phase to the phase where the Higgs doublet obtains a vacuum expecation value. It is, of course, possible that the transition only occurs in the doublet direction. We will identify the regions of parameter space where a two-step transition is possible, and derive a dimensionally-reduced effective theory that can be used to study the EWPT in this model. For numerical analysis, we limit ourselves to the simpler single-step case.

4.1 Full structure of the theory

We write the full symmetric-phase Lagrangian in Euclidean space as

$$\mathcal{L} = \mathcal{L}_{\text{gauge}} + \mathcal{L}_{\text{ghost}} + \mathcal{L}_{\text{GF}} + \mathcal{L}_{\text{fermion}} + \mathcal{L}_{\text{Yukawa}} + \mathcal{L}_{\text{scalar}}, \tag{4.1}$$

where the scalar sector reads

$$\mathcal{L}_{\text{scalar}} = (D_\mu \phi)^\dagger (D_\mu \phi) + \frac{1}{2}(D_\mu \Sigma^a)(D_\mu \Sigma^a) + V(\phi, \Sigma) \tag{4.2}$$

and the potential is given by

$$V(\phi, \Sigma) = -\mu_\phi^2 \phi^\dagger \phi - \frac{1}{2}\mu_\Sigma^2 \Sigma^a \Sigma^a + \lambda(\phi^\dagger \phi)^2 + \frac{b_4}{4}(\Sigma^a \Sigma^a)^2 + \frac{a_2}{2}\phi^\dagger \phi \Sigma^a \Sigma^a. \tag{4.3}$$

Here ϕ is the Higgs doublet and Σ is the SU(2) triplet. Collider experiments at the Large Hadron Collider (LHC) set strong constraints on first-order EWPT scenarios in BSM models involving scalars transforming non-trivially under SU(3) [71, 72]; we therefore omit gluon-Σ couplings. Furthermore, we choose to set the hypercharge of the triplet to zero, so that its covariant derivative reads $D_\mu \Sigma^a = \partial_\mu \Sigma^a + g\epsilon^{abc}A_\mu^b \Sigma^c$.

The potential possesses a global symmetry under $SO(3)_\Sigma$. Adding terms of the form $\phi^\dagger(\Sigma^a T^a)\phi$, where T^a are the SU(2) generators, would break this rotational symmetry and induce a non-zero vev for the neutral triplet component in the broken phase [73]. However, the triplet vev is strongly restricted by electroweak precision tests and has negligible effect on the EWPT in the its allowed value range [52], so we have chosen to discard the $O(3)_\Sigma$ breaking terms from the potential. Furthermore, in Ref. [74] it has been pointed out that the neutral BSM scalar can fit the role of a cold dark matter (CDM) candidate in the absence of a vev. Note that this scalar potential is also symmetric under cyclic group Z_2 transformations:

$$\phi \to -\phi, \quad \Sigma \to -\Sigma. \tag{4.4}$$

We use a simplified Yukawa sector in which only the top quark is coupled to the Higgs doublet, as the other Yukawa couplings are small and insignificant for EWPT. Furthermore, possible fermion couplings to the triplet field would lead to right-handed neutrinos and are generally strongly restricted by experiments [75], so we omit them. Yukawa sector of the Lagrangian reads

$$\mathcal{L}_{\text{Yukawa}} = g_Y(\bar{q}_t \tilde{\phi} t + \bar{t} \tilde{\phi}^\dagger q_t), \tag{4.5}$$

where q_t is the left-handed top quark.

Rest of the theory has the same form as in the SM, but for clarity, we write it down explicitly as well. The gauge fields $A_\mu^a, B_\mu, C_\mu^\alpha$ are contained in the field strength tensors $G_{\mu\nu}^a, F_{\mu\nu}, H_{\mu\nu}^\alpha$. Their respective ghost fields are $\eta^a, \xi, \zeta^\alpha$, and the gauge sector reads

$$\mathcal{L}_{\text{gauge}} = \frac{1}{4} G_{\mu\nu}^a G_{\mu\nu}^a + \frac{1}{4} F_{\mu\nu} F_{\mu\nu} + \frac{1}{4} H_{\mu\nu}^\alpha H_{\mu\nu}^\alpha, \tag{4.6}$$

$$\mathcal{L}_{\text{ghost}} = \partial_\mu \bar{\eta}^a D_\mu \eta^a + \partial_\mu \bar{\xi}^a \partial_\mu \xi + \partial_\mu \bar{\zeta}^\alpha D_\mu \zeta^\alpha, \tag{4.7}$$

$$\mathcal{L}_{\text{GF}} = \frac{1}{2\xi}(\partial_\mu A_\mu^a)^2 + \frac{1}{2\xi}(\partial_\mu B_\mu)^2 + \frac{1}{2\xi}(\partial_\mu C_\mu^\alpha)^2. \tag{4.8}$$

We choose to express the intermediate diagrammatic results for parameter matching using the Landau gauge $\xi = 0$, but emphasize that the final DR relations are gauge invariant. All parameters introduced here are to be understood as the bare parameters; we will discuss renormalization in section 5.

New vertices induced by the triplet and their respective Feynman rules have been listed in Appendix A.

4.2 Triplet model phenomenology

In order to study zero-temperature vacuum structure of the scalar sector, we parametrize the fields as

$$\phi = \begin{pmatrix} \omega^+ \\ \frac{1}{\sqrt{2}}(h + iz) \end{pmatrix}, \quad \Sigma = \begin{pmatrix} \sigma_1 \\ \sigma_2 \\ \sigma_3 \end{pmatrix}, \tag{4.9}$$

where the physical neutral scalars are h and σ_3. The potential possesses multiple stationary points, which can be identified by imposing extremization conditions in neutral component directions,

$$\frac{\partial V}{\partial h} = \frac{\partial V}{\partial \sigma_3} = 0, \tag{4.10}$$

with other components set to zero. We find nine solutions, but due to Z_2 symmetry, only four of these correspond to distinct extrema. Apart from the symmetric phase vacuum at $h = 0, \sigma_3 = 0$, the extrema are given by

$$(h, \sigma_3) = (v, 0) \tag{4.11}$$

$$(h, \sigma_3) = (0, x), \tag{4.12}$$

$$(h, \sigma_3) = \left(\sqrt{\frac{2a_2\mu_\Sigma^2 - 4b_4\mu_\phi^2}{a_2^2 - 4b_4\lambda}}, \sqrt{\frac{2a_2\mu_\phi^2 - 4\lambda\mu_\Sigma^2}{a_2^2 - 4b_4\lambda}} \right), \tag{4.13}$$

where $v = \mu_\phi/\sqrt{\lambda}$ is the usual SM vev and $x = \mu_\Sigma/\sqrt{b_4}$. The first choice corresponds to the standard vacuum of broken electroweak symmetry, given that $\lambda > 0$. Since we restrict the triplet field to real values, the solution $\sigma_3 = x$ is only meaningful if $\mu_\Sigma^2 > 0$.

Mass spectrum in the $(h, \sigma_3) = (v, 0)$ vacuum is found by shifting $h \to h + v$ and diagonalizing the potential. In the absence of aforementioned $O(3)_\Sigma$ breaking terms, there is no mixing between mass eigenstates of ϕ and Σ, and the calculation is straightforward. The four degrees of freedom of ϕ become three Goldstone bosons and the physical Higgs boson of mass

$$m_H^2 = 2\mu_\phi^2 = (125\,\text{GeV})^2. \tag{4.14}$$

The triplet sector is already diagonal with degenerate mass eigenvalues,

$$m_\Sigma^2 = -\mu_\Sigma^2 + \frac{1}{2}a_2 v^2. \tag{4.15}$$

The neutral scalar is given by $\Sigma^0 = \sigma_3$ and σ_1, σ_2 mix to form the charged scalars: $\Sigma^\pm = \frac{1}{\sqrt{2}}(\sigma_1 \mp i\sigma_2)$. Note that at tree level, all three BSM particles have an equal mass of m_Σ. However, loop corrections are different for the neutral and charged scalars, the latter of which obtains additional contributions from its interactions with photons. This leads to a slight splitting of the physical masses by roughly $M_\Sigma^\pm - M_\Sigma^0 = 160$ MeV.

Stability of the EW vacuum requires that $(h, \sigma_3) = (v, 0)$ gives the global minimum, with real mass eigenvalues. A direct calculation shows that the stationary point $h \neq 0, \sigma_3 \neq 0$ does not correspond to a physically meaningful local minimum. Provided that $\lambda > 0$, a stability condition can then be found by requiring that $V(v, 0) < V(0, x)$, which is satisfied for $b_4 > 0$ if

$$\frac{1}{2}m_H^2 v^2 > \frac{1}{b_4}\left(m_\Sigma^2 - \frac{1}{2}a_2 v^2\right)^2 \quad \text{or} \quad \mu_\Sigma^2 < 0. \tag{4.16}$$

If the latter inequality holds, the stationary point in the σ_3 direction is achieved only with complex field values and is ruled out for a real-valued Σ. Furthermore, for the discussion of a two-step phase transition, it is useful to identify regions of the parameter space where the solution $(h, \sigma_3) = (0, x)$ is a local minimum of the potential. This requires[2]

$$\mu_\Sigma^2 > 0 \quad \text{and} \quad \frac{1}{2}m_H^2 < \frac{a_2}{2b_4}\left(\frac{1}{2}a_2 v^2 - m_\Sigma^2\right). \tag{4.17}$$

In particular, the EW vacuum is always stable in the region of a single-step transition.

Finally, measurements of decay widths in collider experiments set additional constraints on the ΣSM parameters. In particular, presence of the charged triplet modifies the observable Higgs-diphoton branching fraction $\Gamma_{H \to \gamma\gamma}$ [52, 73, 76]. In the SM, leading-order contributions to this process come from top quark and W boson loop diagrams. The branching fraction is modified by the portal coupling a_2, and the change in $\Gamma_{H \to \gamma\gamma}$ can be calculated. For sufficiently large values of the triplet mass, small deviations in the branching fraction are currently not excluded by experiments [52, 73]. This may change once the

---

[2]Note that in Ref. [52], there are misprints in both vacuum stability and second minimum conditions.

LHC enters the high luminosity phase, which is expected to allow the determination of $\Gamma_{H\to\gamma\gamma}$ with precision of $\sim 5-10\%$ [77]. Furthermore, the charged triplet can decay into Σ_0 via pion emission, which would leave signatures in charge tracks [73]. Due to the short lifetime of the neutral triplet however, no significant restriction have yet been obtained for this decay [78, 79], and the ΣSM parameter space remains relatively unconstrained by experiments.

4.3   Two step EWBG in the ΣSM

In the SM, EWPT takes place when the Higgs doublet obtains a non-zero vacuum expectation value. When additional scalars are introduced, it becomes possible that the transition is driven by multiple scalars instead of just the SM Higgs. For two scalars transforming non-trivially under the $\mathrm{SU}(2)_L$ group, this scenario is usually modeled in two steps [80]. First, the BSM field undergoes a phase transition by generating a non-zero vev. If this transition is of first order, bubbles of the new phase are formed and baryon creation via sphaleron processes becomes possible. In the second step, the SM doublet settles to its vev of $v = 246$ GeV. The electroweak symmetry is broken already during the first step, causing considerable suppression of B violation in the second step [81]. It is thus preferable to have the baryon excess generated in the first step. For successful baryogenesis, re-excitement of the SM sphalerons in the later step needs then to be avoided, as these could negate the non-zero baryon number of the first step.

In the ΣSM, this scenario has been considered perturbatively in Ref. [52]. In the parameter space spanned by a_2, b_4 and m_Σ, there exists a region of stable EW vacuum where the potential additionally possesses a local minimum in the Σ direction. When thermal corrections to the potential are taken into account, this triplet minimum can become energetically favorable over the symmetric phase vacuum, and the universe can then undergo a transition into the minimum at $(h, \sigma_3) = (0, x)$. As the temperature decreases, the global minimum shifts to the EW vacuum and an another transition occurs. In the model considered in Ref. [52], the triplet vev is relaxed to zero during the second transition, allowing the neutral component become a CDM candidate. Furthermore, it was demonstrated that a first-order transition is achievable for ΣSM couplings within current phenomenological bounds. The perturbative analysis also suggests that in the region of a viable two-step transition, the second step occurs via a strongly first-order transition. This is favorable for baryogenesis, as the expanding bubble walls allow for CP violating scattering processes, preventing a baryon washout by the SM sphalerons. As the existence of a metastable minimum requires $\mu^2 > 0$, a single-step transition is expected in regions not satisfying this condition.

Quantitative estimates concerning the baryon excess produced during a two-step transition in the ΣSM have been left for a future study. For this, non-perturbative methods become essential. We will now apply DR to the ΣSM and describe the resulting 3d theories that can be used for lattice studies of this model.

4.4 Effective 3d theories for the ΣSM

Dimensionally-reduced effective theories for heavy and light scales are constructed as described in section 3, by calculating the relevant correlation functions to order $O(g^4)$ and matching the static Green's functions to those of the underlying theory. Conceptually, DR is made possible by the emergence of a thermal scale hierarchy in the effective field masses; therefore, a scaling assumption for the triplet mass parameter μ_Σ is in order. If the triplet is sufficiently light, its zero-mode will remain in the final effective theory together with that of the doublet field, and this theory can describe a two-step phase transition. However, if the triplet belongs in the "superheavy" or "heavy" category, we may integrate it out in first or second step of DR and obtain the light-scale theory of Eq. (3.23). We may study this case by using the existing lattice results of Ref. [36].

For concreteness, let us write down the 3d theories for different choices of μ_Σ scaling. In a pure SM theory, the field driving the EWPT is the Higgs doublet ϕ, and therefore its mass parameter is assumed to scale at least as $\mu_\phi \sim gT$. After integrating out the superheavy field modes, we obtain a Euclidean 3d theory defined as

$$\mathcal{L}^{(3)} = \mathcal{L}^{(3)}_{\text{gauge}} + \mathcal{L}^{(3)}_{\text{ghost}} + \mathcal{L}^{(3)}_{\text{GF}} + \mathcal{L}^{(3)}_{\text{scalar}} + \mathcal{L}^{(3)}_{\text{temporal}}, \tag{4.18}$$

with the scalar section

$$\mathcal{L}^{(3)}_{\text{scalar}} = (D_r\phi)^\dagger(D_r\phi) + \frac{1}{2}(D_r\Sigma^a)^2 + V(\phi, \Sigma), \tag{4.19}$$

$$V(\phi, \Sigma) = \mu^2_{\phi,3}\phi^\dagger\phi + \frac{1}{2}\mu^2_{\Sigma,3}\Sigma^a\Sigma^a + \lambda_3(\phi^\dagger\phi)^2 + \frac{b_{4,3}}{4}(\Sigma^a\Sigma^a)^2 + \frac{a_{2,3}}{2}\phi^\dagger\phi\Sigma^a\Sigma^a. \tag{4.20}$$

The index r runs from 0 to 3. In order to simplify the notation, we have denoted the 3d fields, defined as in Eq. (3.8), with the same symbol as their 4d counterparts, while 3d couplings are denoted by a subscript. We have now assumed that the triplet is heavy. In the case of a superheavy triplet, even its zero mode has to be integrated out in the first step of DR and so the resulting 3d theory only contains the doublet field. We will not consider this scenario in this thesis; see, however, appendix B of Ref. [53].

The temporal scalars A_0^a, B_0, C_0^α are contained in $\mathcal{L}^{(3)}_{\text{temporal}}$, which reads

$$\begin{aligned}
\mathcal{L}^{(3)}_{\text{temporal}} &= \frac{1}{2}(D_r A_0^a)^2 + \frac{1}{2}m_D^2(A_0^a A_0^a) + \frac{1}{2}(\partial_r B_0)^2 + \frac{1}{2}{m_D'}^2 B_0^2 + \frac{1}{2}(\partial_r C_0^\alpha)^2 + \frac{1}{2}{m_D''}^2(C_0^\alpha C_0^\alpha) \\
&\quad + \frac{1}{4}\kappa_3(A_0^a A_0^a)^2 + \frac{1}{4}\kappa_3' B_0^4 + \frac{1}{4}\kappa_3'' A_0^a A_0^a B_0^2 + h_3(\phi^\dagger\phi A_0^a A_0^a) + h_3'(\phi^\dagger\phi B_0^2) \\
&\quad + h_3'' B_0(\phi^\dagger A_0^a \sigma^a \phi) + \delta_3(\Sigma^a\Sigma^a)(A_0^b A_0^b) + \delta_3'(\Sigma^a A_0^a)^2 + \omega_3 C_0^\alpha C_0^\alpha \phi^\dagger\phi, \tag{4.21}
\end{aligned}$$

where σ_a are the Pauli matrices. Performing parameter matching for the couplings $\kappa_3, \kappa_3', \kappa_3''$ one finds that their leading-order results are $\sim g^4$, so their effects to $O(g^4)$ DR are always of higher order [53, 60]. Furthermore, we have suppressed operators of the form $A_0^a A_0^a C_0^\alpha C_0^\alpha$, $B_0^2 C_0^\alpha C_0^\alpha$ and $(C_0^\alpha C_0^\alpha)^2$, which only contribute at higher orders in our power counting. We have also simplified the SU(3) sector by omitting the gluon coupling to C_0^α. This is because spatial gluons do not couple to the scalars ϕ, Σ, and thus do not contribute to light-scale

matching. Other parts of the Lagrangian are analogous to those defined in section 4.1, with the couplings and fields replaced by their respective 3d counterparts.

In the second step of DR, a light-scale theory is constructed by integrating out the heavy temporal scalars. Near the transition, mass corrections from the first DR step force the doublet mass parameter $\mu_{\phi,3}$ to be light. If a similar cancellation occurs for the triplet, it is justified to include Σ in the light-scale theory as well. We then obtain the theory

$$\bar{\mathcal{L}}^{(3)} = \bar{\mathcal{L}}^{(3)}_{\text{gauge}} + \bar{\mathcal{L}}^{(3)}_{\text{ghost}} + \bar{\mathcal{L}}^{(3)}_{\text{GF}} + \bar{\mathcal{L}}^{(3)}_{\text{scalar}}, \tag{4.22}$$

constructed as described in section 3.4. The scalar sector reads

$$\begin{aligned}
\bar{\mathcal{L}}^{(3)}_{\text{scalar}} = {} & (D_r\phi)^\dagger(D_r\phi) + \frac{1}{2}(D_r\Sigma^a)^2 + \bar{\mu}^2_{\phi,3}\phi^\dagger\phi + \frac{1}{2}\bar{\mu}^2_{\Sigma,3}\Sigma^a\Sigma^a \\
& + \bar{\lambda}_3(\phi^\dagger\phi)^2 + \frac{\bar{b}_{4,3}}{4}(\Sigma^a\Sigma^a)^2 + \frac{\bar{a}_{2,3}}{2}\phi^\dagger\phi\Sigma^a\Sigma^a.
\end{aligned} \tag{4.23}$$

This theory is able to describe a two-step phase transition, since the triplet field is included dynamically. We plan on simulating this theory on the lattice in the near future in order to make non-perturbative statements about the effect the triplet field has on transition dynamics.

However, given the amount of effort required for such simulations, we shall now focus on the simpler case in which the triplet is integrated out as a heavy field. This modifies the matching relations for the light-scale theory, and scalar potential in the final theory is then given by

$$V(\phi) = \hat{\mu}^2_{\phi,3}\phi^\dagger\phi + \hat{\lambda}_3(\phi^\dagger\phi)^2. \tag{4.24}$$

Effects of the triplet field are incorporated into the matching relations for the fields and parameters. We then simplify this theory further by discarding SU(3) and U(1) gauge fields which have little effect on the transition, obtaining the effective theory discussed in section 3.5. Lattice results for this theory are known, and we can obtain non-perturbative results in the limit where the triplet field only affects transition dynamics via its interactions with the doublet. The transition then occurs in a single step driven by the doublet field, from the $\langle\phi\rangle = 0$ symmetric phase directly to the EW vacuum $\langle\phi\rangle = 246$ GeV. In the SM, this transition is of a crossover type. However, the 3d parameters are now modified by the triplet field in a way determined by the matching relations, and the transition may become strong enough to be of first order in some regions of the 4d parameter space.

Matching relations in each of these cases can be found in the main paper [53], while intermediate results of a diagrammatic calculation of the relevant correlation functions are listed in Appendices B and C of this thesis.

5 Technical details of dimensional reduction of the ΣSM

While the construction of the effective theories described above is, in principle, straightforward, there are subtleties that we previously overlooked when describing the matching procedure. In order to produce sensible mappings to the effective 3d theories, a proper renormalization of the 4d theory is required. This subsection is devoted to discussion of technical subtleties related to renormalization of both the full underlying theory as well as the effective theories. Furthermore, the importance of resummation is discussed in detail. We address numerical uncertainties related to dimensionally-reduced effective theories and perform a simple error estimate that can provide insight into the reliability of our results. It is worth pointing out that the techniques presented here can readily be generalized to other scalar extensions of the SM as well.

5.1 One-loop renormalization of the 4d theory

Let us begin with the first step of DR and seek to integrate out the superheavy field modes. As described in section 3.2, calculation of several two and four-point functions is needed to construct parameter mappings to the 3d theory. Remarkably, it is enough to compute only the contributions from superheavy Matsubara modes, as the diagrams containing solely light and heavy modes are reproduced by the 3d theory and need not be matched. For now, we will assume that the triplet field is heavy; superheavy contributions then come from bosonic $n \neq 0$ modes and all fermionic modes.

We apply the $\overline{\text{MS}}$ renormalization scheme in $D = 4 - 2\epsilon$ dimensions and define the bare fields and parameters as

$$\phi_{i,(b)} = Z_{\phi_i}^{1/2}\phi_i = (1 + \delta Z_{\phi_i})^{1/2}\phi_i \quad \text{(for gauge, fermion and scalar fields)}, \tag{5.1}$$

$$g_{i,(b)} = \Lambda^\epsilon(g_i + \delta g_i) \quad \text{(for gauge couplings)} \tag{5.2}$$

and

$$y_{t,(b)} = Z_\phi^{-\frac{1}{2}}Z_q^{-\frac{1}{2}}Z_u^{-\frac{1}{2}}\Lambda^\epsilon(g_Y + \delta g_Y), \qquad \lambda_{(b)} = Z_\phi^{-2}\Lambda^{2\epsilon}(\lambda + \delta\lambda), \tag{5.3}$$

$$b_{4,(b)} = Z_\Sigma^{-2}\Lambda^{2\epsilon}(b_4 + \delta b_4), \qquad a_{2,(b)} = Z_\phi^{-1}Z_\Sigma^{-1}\Lambda^{2\epsilon}(a_2 + \delta a_2), \tag{5.4}$$

$$\mu_{\phi,(b)}^2 = Z_\phi^{-1}(\mu_\phi^2 + \delta\mu_\phi^2), \qquad \mu_{\Sigma,(b)}^2 = Z_\Sigma^{-1}(\mu_\Sigma^2 + \delta\mu_\Sigma^2). \tag{5.5}$$

Here Λ is the renormalization group (RG) scale, and its inclusion in bare coupling definitions makes the renormalized couplings dimensionless. Technically, all $O(g^4)$ Feynman diagrams then come with a factor of $\Lambda^{4\epsilon}$, but we absorb it into the integration measure by introducing the shorthand notation

$$\int_p \equiv \left(\frac{e^\gamma \Lambda^2}{4\pi}\right)^\epsilon \int \frac{d^d p}{(2\pi)^d}, \tag{5.6}$$

where $d = 3 - 2\epsilon$. Note that due to broken Lorentz invariance, dimensionality of the temporal direction is exactly one, while the spatial space is d-dimensional. As usual in dimensional regularization, all integrals encountered are at most logarithmically divergent.

$O(g^4)$ matching relations for the coupling constants are obtained from one-loop corrections to their respective vertices. For example, matching of the SU(2) gauge coupling g is readily performed by calculating the $\phi^\dagger \phi A_\mu^a A_\nu^b$ correlator. It contains the ring diagram depicted in Fig. 2, which is proportional to the sum-integral

$$\sum\!\!\!\!\!\!\!\int_P \frac{1}{(P^2 + \mu_\Sigma^2)^2}. \tag{5.7}$$

As pointed out in section 2.1, we can now separate the above expression into a zero-mode part and a sum-integral over all $n \neq 0$ modes. The zero-mode contribution is reproduced by the 3d theory and is not needed for the construction of the DR mapping. For heavy μ_Σ, we may simplify these integrals by expanding in $\mu_\Sigma^2/T^2 \sim g^2$ in the $n \neq 0$ part:

$$\sum\!\!\!\!\!\!\!\int_P'\frac{1}{(P^2 + \mu_\Sigma^2)^2} = \sum\!\!\!\!\!\!\!\int_P'\frac{1}{P^4} + \mu_\Sigma^2 \sum\!\!\!\!\!\!\!\int_P'\frac{1}{P^6} + O(g^8), \tag{5.8}$$

where it is sufficient to only pick the zeroth-order term, since the diagram itself is proportional to g^4 and thus any positive powers of μ_Σ lead to corrections beyond $O(g^4)$. Note that a similar expansion is not allowed for zero-mode propagators as each term in the resulting expansion would vanish in dimensional regularization, leading to a wrong result [63].
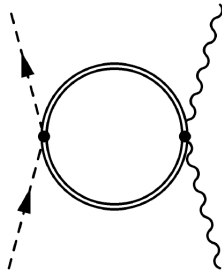
Figure 2: Ring diagram containing a Σ loop. For spatial A_μ, this diagram cancels against a triangle diagram at $O(g^4)$, and the temporal part contributes only to the matching relation for the $\phi - A_0$ portal coupling h_3.

Under the assumption that all mass parameters appearing in the theory scale at least as $\sim gT$, we can follow the recipe introduced above to reduce all other integrals appearing in the four-point function to bosonic sum-integrals of the form

$$I_{\alpha,\beta,\delta}^{4b} \equiv \sum\!\!\!\!\!\!\!\int_P'\frac{(P_0^2)^\beta (\mathbf{p}^2)^\delta}{(P^2)^\alpha}, \tag{5.9}$$

which can further be simplified using common algebra (see the list of integrals in Ref. [60]). A direct computation then shows that for spatial A_μ, the diagram in Fig. 2 cancels against a triangle diagram of the same type at $O(g^4)$. Two particularly important one-loop sum-integrals are [35, 61]

$$I_1^{4b} \equiv \sum\!\!\!\!\!\!\!\int_P'\frac{1}{P^2} = \frac{T^2}{12}\left\{1 - \epsilon L_b - 4\epsilon\left(c + \ln\frac{3T}{\Lambda}\right)\right\} + O(\epsilon^2), \tag{5.10}$$

$$I_2^{4b} \equiv \sum\!\!\!\!\!\!\!\int_P'\frac{1}{P^4} = \frac{1}{16\pi^2}\left(\frac{1}{\epsilon} + L_b\right) + O(\epsilon), \tag{5.11}$$

where logarithms of Λ are contained in L_b as defined in Eq. (3.14), and we have denoted

$$c \equiv \frac{1}{2}\left(\ln\left(\frac{8\pi}{9}\right) + \frac{\zeta'(2)}{\zeta(2)} - 2\gamma\right). \tag{5.12}$$

The $O(\epsilon)$ terms are important for two-loop renormalization of two-point functions where products of the above sum-integrals appear. Note in particular that at one-loop, logarithms of the form $\ln(\Lambda^2/T^2)$ always come with the same coefficient as the corresponding UV-divergent $1/\epsilon$ term. This is a reflection of the fact that UV and IR divergences cancel each other in dimensional regularization, as the role of an IR regulator is played here by T. The counterterm δg is defined, as usual, to exactly cancel the $1/\epsilon$ poles arising from these sum-integrals, and the renormalized four-point function is what enters the matching relations. Note, however, that an additional computation and renormalization of the respective two-point functions are needed to obtain the correct field normalization relations.

In the ΣSM, δg is given by

$$\delta g = -\frac{g^3}{16\pi^2\epsilon}\left(\frac{41}{12} - \frac{2}{3}N_f\right), \tag{5.13}$$

where $N_f = 3$ is the number of fermion families and we have separated it from the bosonic contributions for convenience. Using this, one is able to find the corresponding β-function by requiring that the bare parameter $g_{(b)}$, defined in Eq. (5.2), is independent of Λ. The $O(g^4)$ result reads

$$\beta(g) = -\frac{g^3}{16\pi^2}\left(\frac{41}{6} - \frac{4}{3}N_f\right). \tag{5.14}$$

The β-functions are needed to account for running when studying dimensionally-reduced effective theories. A full list of one-loop counterterms in the ΣSM is presented in Appendix D, while the β-functions can be found in the main paper [53].

After calculating the relevant correlator functions in the ΣSM, one finds the $O(g^4)$ matching relation for g_3:

$$g_3^2 = g(\Lambda)^2 T\left[1 + \frac{g^2}{16\pi^2}\left(\frac{41}{6}L_b(\Lambda) - \frac{4N_f}{3}L_f(\Lambda) + \frac{2}{3}\right)\right]. \tag{5.15}$$

Running of g^4 is of higher order and we have simplified the notation to reflect this fact. Note that the total coefficient of the $\ln(\Lambda^2/T^2)$ term is exactly the renormalization group equation $\beta(g^2) = 2g\beta(g)$ with its sign flipped. This is because the only UV-divergent sum-integral we face at one-loop level is I_2^{4b}, and therefore all emerging logarithmic Λ dependence is equal to the $1/\epsilon$ poles. What this implies is that any Λ dependence in the $O(g^2)$ term will cancel against the logarithmic term, rendering the 3d coupling independent of Λ at $O(g^4)$. This is a general result that reflects the super-renormalizable nature of the effective theory, and applies to all coupling constants in the matched theory [34, 35, 82].

A remarkable result of thermal field theory is that a Wick rotation from vacuum to an Euclidean finite-temperature theory preserves the ultraviolet behavior of the theory. The omitted zero-mode integrals at one-loop level are all UV-finite (see section 5.3), implying

that the one-loop counterterms calculated from the superheavy diagrams are sufficient to renormalize the corresponding vacuum theory as well. This comes in handy when considering loop corrections to relations between physical and $\overline{\text{MS}}$ parameters, discussed in section 5.5.

5.2   Two-loop mass parameter matching

Matching becomes more complicated at two-loop level. It is still useful to decompose bosonic sum-integrals into purely zero-mode contributions and $n \neq 0$ mode sum-integrals, but one also gets mixed terms:

$$\sumint_{P,K} = T^2 \int_{p,k} + T \sumint_P' \int_k + T \sumint_K' \int_p + \sumint_{P,K}' . \qquad (5.16)$$

Again, the zero-mode term proportional to T^2 corresponds to a 3d integral and has a direct counterpart in the effective theory, while the terms linear in T turn out to be irrelevant for parameter matching (for details, see section 5.4). Finally, the last contribution consisting only of non-zero mode momenta is what enters the matching relations for mass parameters. The total two-point function is renormalized by $O(g^4)$ counterterm diagrams containing one-loop counterterms. However, at two-loop level even the purely zero-mode 3d integrals can be UV divergent, and one would find an excess of logarithmic divergence if attempting to renormalize only the supermassive contributions. This leftover divergence cancels exactly against the remaining UV divergence in the zero-mode parts, and the total correlator is thus UV finite. In fact, this observation allows one to find the $O(g^4)$ result for the mass counterterm of the effective 3d theory in terms of parameters of the 4d theory.

Integrals relevant for two-loop DR can be found in Ref. [60], and remarkably, all $n \neq 0$ mode contributions can be expressed as products of the integrals in Eq. (5.10), from which we can deduce the UV structure of the scalar self-energy functions. Two-loop diagrams, as well as one-loop counterterm diagrams, therefore produce logarithms of the type $\ln(3T/\Lambda)$ that were not present in one-loop calculations. These logarithms correspond to two-loop running, and their RG-scale dependence cannot be canceled by one-loop β functions.

Renormalized mass parameters of the heavy scale theory are obtained from Eq. (3.9). One-loop diagrams now produce $O(g^4)$ terms proportional to mass squared when the integrals are expanded as in Eq. (5.8); these lead to logarithmic terms of the form $\mu^2 L_b(\Lambda)$, where μ denotes a general heavy mass. Similar terms are also produced by the one-loop field normalization correction $\bar{\Pi}'(0)$, which is proportional to I_2^{4b} on dimensional grounds. As in coupling constant matching, this implies that the one-loop logarithmic structure corresponds to the UV divergence of these terms, and the Λ dependence is cancelled by running of the tree-level term. Finally, note that L_b cancels in the product $I_1^{4b} I_2^{4b}$. This means that terms of the form $T^2 L_b$ emerge from counterterm diagrams and $O(g^4)$ parts of one-loop diagrams, but not from two-loop diagrams. We can therefore write down the

general structure for the matched mass parameters:

$$\mu_3^2(\Lambda) = -\mu^2(\Lambda) + \left(T^2 f_1(\Lambda)\right)_{O(g^2)}$$
$$+ \left(\beta(\mu^2)L_b(\Lambda) + T^2\left\{f_2 + f_3 L_b(\Lambda) + f_4\left(\ln\frac{3T}{\Lambda} + c\right)\right\}\right)_{O(g^4)}, \qquad (5.17)$$

where the f_i are functions of the couplings and only the running of f_1 is of $O(g^4)$, canceling exactly the Λ dependence of the $T^2 L_b$ terms originating from one-loop diagrams. Note the that we have accounted for the sign difference in mass parameter definitions.

As opposed to the 3d couplings, μ_3^2 by itself will generally not be Λ invariant. This is because of the two-loop logarithms discussed earlier, and reflects the fact that 3d theory requires renormalization at two-loop level. However, the 3d bare mass parameter, defined as

$$\mu_{3,(b)}^2 = \mu_3^2 + \delta\mu_3^2 \qquad (5.18)$$

is independent of the renormalization procedure of either theories and ought to be RG invariant. This statement is physically justified, as the bare mass parameter corresponds to a screening mass similar to the Debye masses and bears physical meaning [83]. This implies that running of the counterterm $\delta\mu_3^2$ must match that of the $\ln(3T/\Lambda)$ terms.

The counterterm can be calculated to $O(g^4)$ accuracy in the 4d theory either by directly computing the contributions from Matsubara zero modes, or by looking at the leftover divergence in the superheavy contributions. It is of the form

$$\delta\mu_3^2 = \frac{T^2}{4\epsilon}\Delta_{4d}, \qquad (5.19)$$

where Δ_{4d} is an $O(g^4)$ function of the couplings. Naively, one might think that its running is of higher order, but this is only true in the limit $\epsilon \to 0$. To be more specific, the ϵ-dependent scaling of the couplings in Eq. (5.3) induces $O(\epsilon)$ running: For gauge and Yukawa couplings we find $\Lambda\frac{d}{d\Lambda}g_i \sim -\epsilon g_i + O(\epsilon^0)$, while the quartic couplings run as $\Lambda\frac{d}{d\Lambda}\lambda \sim -2\epsilon\lambda + O(\epsilon^0)$. The $O(g^4)$ running of $\delta\mu_3^2$ is therefore

$$\Lambda\frac{d}{d\Lambda}\delta\mu_3^2 = -T^2\Delta_{4d}, \qquad (5.20)$$

and Eq. (5.18) is RG invariant at $O(g^4)$ if running of the two-loop logarithms in Eq. (5.17) is cancelled by this running of the counterterm, i.e, if $\Delta_{4d} = -f_4$. This can be verified by directly calculating the zero-mode contributions. By doing so, one indeed finds that the bare 3d mass is independent of Λ by construction.

Strictly speaking, DR is only valid when the logarithmic corrections are small [34, 82]. With the choice $\Lambda = 4\pi T e^{-\gamma} \sim 7T$, all one-loop logarithms can be set to zero. We shall next discuss how super-renormalizability of the effective theory can be used to increase the accuracy of two-loop matching.

5.3   Renormalization of the effective theories

UV divergences in the 3d theories arise at two-loop level and renormalization of the heavy-scale theory is required for $O(g^4)$ mass parameter matching to the light-scale effective theory. Application of the $\overline{\text{MS}}$ scheme in three dimensions introduces a new renormalization scale Λ_3 that *is independent of the RG-scale Λ in the underlying theory.* This follows from the fact that the bare 3d parameters are explicitly RG-invariant with respect to Λ at order $O(g^4)$ [35].

The reduced amount of spacetime dimensions guarantees that all one-loop diagrams are UV finite [83]. To see this, consider an integral of the type

$$\int \frac{d^3 p}{(p^2 + m^2)^n} \tag{5.21}$$

and averaging it over angles. UV behavior of the resulting integral is $\int d^3 p / p^{2n}$, which converges for $n \geq 2$ and for $n = 1$ gives a power divergence that vanishes in dimensional regularization. This suggests that no renormalization is needed for the couplings nor the fields. In order to give the couplings an integer dimension in dimensional regularization, we nevertheless scale them as in Eq. (5.3), with the counterterms set to zero and Λ replaced by the 3d scale Λ_3.

Mass divergences in this effective theory are artifacts of the matching process in which the superheavy scale is integrated out. We have already defined the bare mass parameter $\mu_{3,(b)}^2$ in Eq. (5.18), and pointed out that it can be calculated in the 4d theory to $O(g^4)$ accuracy. However, due to super-renormalizability, it is possible to include higher order corrections by computing it directly in the effective theory. The mass counterterms are especially important for 3d lattice analyses, as they can be used in calculation of discretized counterterms for substracting lattice divergences.

By calculating the UV divergence to order $O(g_3^4)$, one finds

$$\delta \mu_3^2 = \frac{1}{4\epsilon} \Delta_{\text{3d}}, \tag{5.22}$$

which is equal to Eq. (5.19) up to higher-order corrections in g. As the 3d couplings only have $O(\epsilon)$ running, solving the RG equation for μ_3^2 is trivial. Integration over Λ_3 produces a constant mass scale Λ_0, and the mass parameter reads

$$\mu_3^2 = -\Delta_3 \ln \left(\frac{\Lambda_0}{\Lambda_3} \right) + \text{constant}. \tag{5.23}$$

Λ_0 can be fixed by comparing this expression against the full matching relation for μ_3^2, computed in terms of 4d parameters in Eq. (5.17). In the previous section we argued that invariance with respect to the 4d RG scale requires the running of the counterterm to cancel that of the two-loop logarithms. The $O(g^4)$ counterpart of the logarithm in Eq. (5.23) is therefore the term $f_4 \big(\ln 3T/\Lambda + c \big)$, and we deduce that

$$\Lambda_0 = 3Te^c \approx 2.1T. \tag{5.24}$$

The matching relation for μ_3^2 thus defines an initial condition for the RG equation of the 3d theory.

Note that both the mass counterterm and the RG equation are exact quantities due to the super-renormalizable nature of the theory and receive no corrections at higher orders of perturbation theory [34]. We can use this information to our advantage by performing the parameter matching at scale $\Lambda_3 = \Lambda$ and replacing the two-loop logarithmic term in the matching relation by its higher-order corrected value, given by Eq. (5.22). This discussion demonstrates that the structure of the matching relations is determined in a non-trivial way by RG equations of both the 4d and 3d theories.

5.4 Resummation in DR

When we described construction of the heavy-scale theory in section 3.2, it was essential to be able to separate the 4d correlation functions into a static 3d part and a contribution from the superheavy modes, denoted $\bar{\bar{\Pi}}$. In order to match the off-shell Green's functions, it was then assumed that the static contribution, corresponding to diagrams that only contain light or heavy propagators, could be directly matched to the full correlation function of the 3d theory. There is a complication, however, since the masses entering the propagators are different in the two theories. The importance of this statement becomes explicit when considering diagrams containing gauge fields. In 4d, the $\langle \phi^\dagger \phi \rangle$ correlator obtains a contribution from the gauge bubble diagram depicted in Fig. 3a. Since gauge fields are massless in the symmetric phase, the $n = 0$ portion of this diagram vanishes in dimensional regularization. However, in the 3d theory the gauge fields only have three components, and to compensate for this, there exist additional massive scalars that are not present in the 4d theory. The corresponding 3d diagrams are shown in Fig. 3b, and the A_0 contribution is non-vanishing due to the propagator containing a mass scale. The mass in question is exactly the Debye mass, generated in the temporal component by screening effects. The contribution from this diagram is not present in the 4d theory, and it seems like the matching procedure has failed.

The above discussion demonstrates the need for a systematic method for distinguishing between diagrams that are reproduced by the 3d theory and those that are not, the latter of which contribute to the parameter matching. This becomes even more important at two-loop level where the integrals can contain mixed $n = 0$ and $n \neq 0$ field modes. The formal way of identifying the 3d contributions is to use the resummation method of Arnold and Espinosa [84]. For all fields appearing in both the 4d and the 3d theory, we explicitly add and subtract thermal mass terms for their Matsubara zero-modes in the 4d Lagrangian. For example,

$$\frac{1}{2}\mu_\Sigma^2 \Sigma^a(0,\mathbf{p})\Sigma^a(0,\mathbf{p}) = \frac{1}{2}\underline{\mu}_\Sigma^2 \Sigma^a(0,\mathbf{p})\Sigma^a(0,\mathbf{p}) - \frac{1}{2}\bar{\Pi}_\Sigma \Sigma^a(0,\mathbf{p})\Sigma^a(0,\mathbf{p}), \qquad (5.25)$$

where $\underline{\mu}_\Sigma^2 \equiv \mu_\Sigma^2 + \bar{\Pi}_\Sigma$ is called a resummed mass and enters the propagator, while $\bar{\Pi}_\Sigma$ is the squared thermal mass of the triplet field, corresponding to a loop correction from the $n \neq 0$ modes to the two-point correlator. Similar procedure is carried out for the doublet field. The term $-\frac{1}{2}\bar{\Pi}_\Sigma \Sigma^a(0,\mathbf{p})\Sigma^a(0,\mathbf{p})$ is treated as an interaction, producing
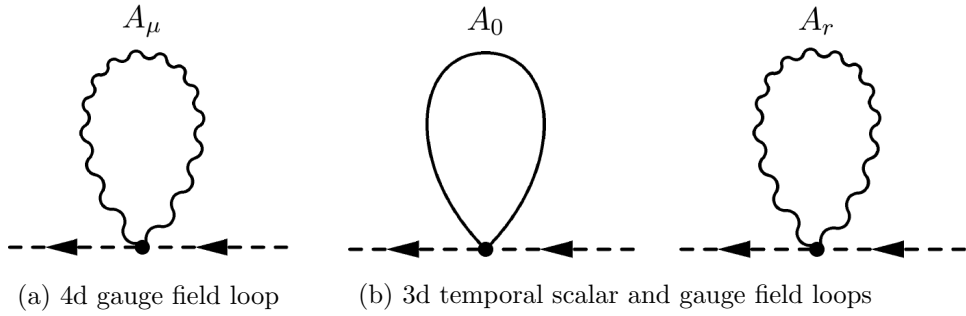
(a) 4d gauge field loop   (b) 3d temporal scalar and gauge field loops

Figure 3: A 4d diagram that is screened into two separate diagrams in the 3d theory. The scalar contribution needs to be separated in the 4d diagram in order to match the two-point functions.

additional vertices in perturbation theory. For this reason, we refer to terms of the form $-\bar{\Pi}_\Sigma$ as "thermal counterterms", despite being both UV and IR finite. For gauge fields in particular, resummation is only performed for the temporal component by adding and subtracting the term $m_D A_0^a(0, \mathbf{p}) A_0^a(0, \mathbf{p})$ for the SU(2) field, and similarly for B_0 and C_0. This introduces a term of the form $1/(\mathbf{p}^2 + m_D^2)$ in the $n = 0$ mode propagator, generating the contribution that was previously seemingly missing from the 4d theory.

The thermal counterterms have a subtle effect on the construction of the matching relations. The tree-level interaction diagram will just cancel the added term in the resummed propagator, but at $O(g^4)$, the thermal counterterms appear also in one-loop diagrams contributing to self-energies. Recall that a general two-loop sum-integral can be written as in Eq. (5.16). The thermal counterterm diagrams are proportional to $T\bar{\Pi}$ times a resummed 3d integral and their added effect is to cancel the mixed $n = 0$ and $n \neq 0$ contributions linear in T from the sum-integrals [35, 84]. This is the reason for neglecting these terms from parameter matching in the previous section. The mixed terms are problematic due to the zero-mode propagators that can cause IR divergences. The fact that they can be canceled by reorganizing the perturbative expansion indicates that the linear terms do not contribute to physical screening effects.

The main advantage of DR over the perturbative 4d effective potential approach lies in the handling of IR divergences. The resummation described here shows explicitly that integration over the superheavy scale is completely IR safe, despite being perturbative in nature. The inevitable IR problems have been included into the 3d theory where their effects are easier to study. To see the cancellation of the linear terms, it suffices to compute the thermal masses at one-loop level. Ultimately, the outcome is that only the purely $n \neq 0$ modes are needed for DR, and resummed masses do not enter the matching relations. In fact, as long as one knows which diagrams contribute to matching, it is possible to ignore this procedure completely, calculating only the relevant contributions. It is, however, useful to verify the cancellation explicitly by performing resummation as described here.

When integrating out heavy fields in the second DR step, similar considerations are in order to identify contributions that are reproduced by the light-scale theory. If a field has a counterpart at light scale, a mass correction is introduced in the heavy-scale Lagrangian.

For the Higgs doublet specifically,

$$\mu_{\phi,3}^2 \phi^\dagger \phi = \underline{\mu}_{\phi,3}^2 \phi^\dagger \phi - \bar{\Pi}_{\phi,3} \phi^\dagger \phi, \tag{5.26}$$

and the triplet field is treated similarly in the case of a light $\mu_{\Sigma,3}$. $\bar{\Pi}_{\phi,3}$ is again computed from the two-point correlator, and a one-loop evaluation is sufficient. New diagrams generated by $-\bar{\Pi}_{\phi,3} \phi^\dagger \phi$ cancel two-loop contributions proportional to $1/\mu_{\phi,3}$, which would otherwise cause IR divergences near the phase transition. Again, construction of the light-scale theory is thus free of IR problems. The resulting effective theory can then be discretized and studied non-perturbatively on the lattice, avoiding IR divergences completely.

5.5 Loop corrections to $\overline{\text{MS}}$ parameters

In the $\overline{\text{MS}}$ scheme, mass parameters and couplings of the full 4d theory are explicitly RG-scale dependent and do not reflect any on-shell physics by themselves. They nevertheless are indispensable for DR, as the whole point is the matching of off-shell Green's functions. We therefore need to relate the $\overline{\text{MS}}$ parameters to measurable quantities, such as physical masses and charges. At tree-level, this is done by bringing the broken-phase Lagrangian into a mass-diagonal basis as in section 4.2. Inverting the mass eigenvalue relations, we obtain

$$\mu_\phi^2 = \frac{1}{2} m_H^2, \tag{5.27}$$

$$\mu_\Sigma^2 = -m_\Sigma^2 + 2 \frac{a_2}{e^2} \frac{m_W^2}{m_Z^2} (m_Z^2 - m_W^2), \tag{5.28}$$

$$\lambda = \frac{e^2}{8} \frac{m_H^2 m_Z^2}{m_W^2 (m_Z^2 - m_W^2)}, \tag{5.29}$$

$$y_t^2 = \frac{e^2}{2} \frac{m_t^2 m_Z^2}{m_W^2 (m_Z^2 - m_W^2)}, \tag{5.30}$$

$$g^2 = e^2 \frac{m_Z^2}{m_Z^2 - m_W^2}, \tag{5.31}$$

$$g'^2 = e^2 \frac{m_Z^2}{m_W^2} \tag{5.32}$$

where m_t, m_W, m_Z are the tree-level masses of the top quark and the W and Z bosons, respectively. e is the elementary charge unit, related to the fine-structure constant α as $e^2 = 4\pi\alpha$.

However, matching the $\overline{\text{MS}}$ parameters only at tree-level can lead to significant errors in the matching relations if couplings and masses are allowed to be large. Loop corrections to the above relations are thus necessary for reliable results – see section 6.2 for comparison. These are achieved by a perturbative calculation of pole masses in the phase of broken SU(2) symmetry, where particle masses are measured. This computation can be performed in Minkowski space at zero temperature, as definitions of the $\overline{\text{MS}}$ parameters are T-independent. For convenience, we choose to use the Feynman gauge in this calculation, since the resulting physical quantities are independent of the choice of gauge.

By definition, the mass of a particle is given by the pole of its propagator, and experimentally determined masses correspond to pole masses computed to an infinite order in perturbation theory. Loop-corrected propagators for the physical particles read

$$\langle h(-p)h(p)\rangle = \frac{i}{p^2 - m_H^2 - \Pi_H(p^2)}, \tag{5.33}$$

$$\langle \Sigma^{0/\pm}(-p)\Sigma^{0/\pm}(p)\rangle = \frac{i}{p^2 - m_\Sigma^2 - \Pi_{\Sigma^{0/\pm}}(p^2)}, \tag{5.34}$$

$$\langle W_\mu(-p)W_\nu(p)\rangle = \frac{g_{\mu\nu}}{p^2 - m_W^2 - \Pi_W(p^2)}, \tag{5.35}$$

$$\langle Z_\mu(-p)Z_\nu(p)\rangle = \frac{g_{\mu\nu}}{p^2 - m_Z^2 - \Pi_Z(p^2)}, \tag{5.36}$$

$$\langle t_\alpha(p)\bar{t}_\beta(p)\rangle = \left[\frac{i}{\not{p} - m_t^2 - \not{p}\Sigma_v(p^2) - \not{p}\gamma_5\Sigma_a(p^2) - m_t\Sigma_s(p^2)}\right]_{\alpha\beta}. \tag{5.37}$$

The Π functions now obtain corrections from reducible tadpole diagrams in addition to the usual 1PI diagrams. This is a general feature of theories with spontaneously broken symmetries [85, 86]. For a consistent $O(g^4)$ analysis, the loop corrections need to be calculated at one-loop order, and proper renormalization needs to be implemented [35]. Note that since the UV behavior is the same both in vacuum and at finite temperature, we may use the one-loop counterterms that were previously calculated for DR.

Denoting the physical masses by capital M, we obtain pole conditions for bosons in the form

$$M_i^2 - \text{Re}[m_i^2 + \Pi_H(M_i^2)] = 0. \tag{5.38}$$

For the fermionic propagator, the situation is somewhat more complicated as the self-energy consists of independent axial, vector and scalar parts. The pole condition is

$$\bar{u}(p)\left[\not{p} - m_t^2 - \not{p}\Sigma_v(p^2) - \not{p}\gamma_5\Sigma_a(p^2) - m_t\Sigma_s(p^2)\right]u(p)\bigg|_{p^2=M_t^2} = 0, \tag{5.39}$$

where $u(p)$ is an asymptotic spinor satisfying the Dirac equation. Using the Gordon decomposition identity

$$\bar{u}(p)\not{p}u(p) = \bar{u}(p)\frac{p^2}{M_t}(p), \tag{5.40}$$

we find

$$M_t^2 = m_t^2(1 + 2\Sigma_s + 2\Sigma_v). \tag{5.41}$$

Note that the axial Σ_a does not contribute to the pole mass.

From the pole conditions we can solve loop-corrections to the mass eigenvalues. In section 4.2 we stated that the triplet field has three mass eigenstates with the eigenvalue m_Σ being degenerate. The loop corrections are, however, slightly different for neutral and charged scalars, and we choose to write the $\overline{\text{MS}}$ parameter μ_Σ in terms of the correction

to the neutral scalar mass. Pole masses are measured at the scale of weak interactions, so the Π functions and α should be evaluated at $\Lambda = m_Z$, with the exception of the top Yukawa coupling, which is evaluated at $\Lambda = M_t$. Substituting these into Eqs. (5.27)-(5.32) gives $O(g^4)$ corrected expressions for the $\overline{\text{MS}}$ parameters. They have been listed in the main paper [53]. Note that loop corrections to the ΣSM parameters a_2 and b_4 need not be calculated as their values have not been determined experimentally, and we can treat their input values as corresponding directly to their values at scale $\Lambda = M_Z$.

5.6   Error estimates from omitted higher-dimension operators

Effective theories always come with intrinsic uncertainties, and error estimates should be provided to address the reliability of the DR procedure. Errors arise both from higher-order contributions to parameter matching, as well as from effective higher-order operators that have not been explicitly matched. These correspond to n-point operators of the form O_n/T^n that are generated when performing integrations over fields. Provided that the couplings are small enough for perturbation theory to be applicable, the leading-order error comes from omitted dimension-six operators. In principle, the effects of these operators could be included in the effective theories by calculating six-point functions in the underlying theory and matching them into the 3d coefficients. A comprehensive estimation of the error caused by neglecting these corrections is generally a non-trivial task. In this section, we present rough estimates for reliability of DR based on the analysis in Ref. [35], and derive an expression for the leading-order error in the ΣSM that can be used to estimate the validity of our EWPT study.

Inclusion of higher-order operators allows for a simple power-counting estimate of the accuracy at which the Green's functions are reproduced. For example, consider introducing an operator of the form $\Omega_6 \phi^\dagger \phi (A_0^a A_0^a)^2$ in the heavy-scale effective theory. Note that dimensionality of this operator is three and the coefficient Ω_6 is dimensionless. In the 4d theory, an effective six-point operator is generated via loop corrections to the $\langle \phi^\dagger \phi (A_0^a A_0^a)^2 \rangle$ six-point function. Denoting the leading-order correction by $\bar{\bar{\Pi}}_6 \sim g^6$, we can perform matching for the 3d parameter Ω_6 just as we would match quartic couplings. The effective vertices are matched as

$$\Omega_6 (\phi^\dagger \phi (A_0^a A_0^a)^2)_{3d} = \frac{1}{T} \bar{\bar{\Pi}}_6(0) \frac{(\phi^\dagger \phi (A_0^a A_0^a)^2)_{4d}}{T^2}, \qquad (5.42)$$

and the $O(g^4)$ result is just $\Omega_3 = \bar{\bar{\Pi}}_6$. The six-point operator now generates new diagrams in the heavy-scale theory. In particular, new contributions to the $\langle \phi^\dagger \phi \rangle$ correlator are dominated by the diagram

$$\sim \Omega_6 \int_{pk} \frac{1}{p^2 + m_D^2} \frac{1}{k^2 + m_D^2}, \qquad (5.43)$$

which is scales as $g^6 m_D^2 \sim g^8$. The 3d mass parameter squared $\mu_{\phi,3}^2$, produced by matching of Green's functions, is of order $g^4 T^2$. We therefore estimate that the relative error in the reproduced Green's functions of the heavy-scale theory is of $O(g^4)$.

We would now like to address the accuracy at which our DR is able to describe the EWPT. For this, consider the six-point operator $\Lambda_6 (\phi^\dagger \phi)^3$ at heavy-scale. The coefficient Λ_6 can be matched to the one-loop corrected six-point function $\langle (\phi^\dagger \phi)^3 \rangle$ in the 4d theory by $\Lambda_6 = \bar{\Pi}_6^\phi(0)$. The value of this loop correction is most conveniently obtained from the one-loop effective potential. In the ΣSM, the result is [53]

$$\Lambda_6 = \frac{\zeta(3)}{16384\pi^4}\left(3g^6 + g'^6 + 3g^2 g'^2(g^2 + g'^2) + 640\lambda^3 - 224y_t^6 + 8a_2^3\right). \tag{5.44}$$

In Ref. [35], the effect of dimension-six operators has been estimated by calculating the relative shift these operators cause to the Higgs vev in the final effective theory. In the minimal SM, the leading-order contribution to the $(\phi^\dagger \phi)^3/T^2$ operator comes from the top quark and causes an error of roughly one percent in the vev. In the ΣSM, there is an additional contribution proportional to a_2^3, and we can estimate its effect by comparing it against the top quark term in Eq. (5.44).

However, dominant BSM contributions to the higher-dimension operators are obtained from integrating out the triplet field as a heavy degree of freedom in the second step of DR. We may include an operator of the form $\bar{\Lambda}_6 (\phi^\dagger \phi)^3$ in the final light-scale theory and match it to the corresponding six-point function at heavy scale. At $O(g^6)$, we find simply that

$$\bar{\Lambda}_6 = \Lambda_6 + \Lambda_6^{\text{heavy}}, \tag{5.45}$$

where one-loop corrections from the triplet and temporal scalars are contained in Λ_6^{heavy}. Errors caused by the temporal scalars are subdominant relative to that of the top quark in the first DR step [35]. In the ΣSM, there is a new contribution to $\bar{\Lambda}_6$, coming from the diagram depicted in Fig. 4. By a direct calculation, we find that the heavy triplet contributes as

$$\Lambda_6^{\text{heavy, BSM}} = \frac{1}{512\pi}\left(\frac{a_{2,3}}{\mu_{\Sigma,3}}\right)^3, \tag{5.46}$$

which scales parametrically as $\sim g^3$.

In our analysis, this heavy-scale contribution generally dominates over the effective coupling Λ_6, obtained in the first step. We therefore identify Eq. (5.46) as the dominant source of errors in our DR procedure. The relative shift caused to the Higgs vev can be approximated by comparing the dominant BSM term to the top quark contribution,

$$\Lambda_6^t = -\frac{7\zeta(3)}{512\pi^4}y_t^6, \tag{5.47}$$

and we define

$$\Delta_6 = \left|\frac{\Lambda_6^{\text{heavy, BSM}}}{\Lambda_6^t}\right|. \tag{5.48}$$
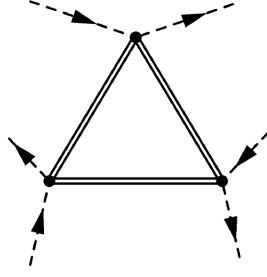
Figure 4: 3d diagram providing a dominant contribution to the omitted light-scale operator $(\phi^\dagger\phi)^3_{3d}$ when the triplet is integrated out.

If this ratio is large in some region of the parameter space, we can expect severe uncertainties in our results within this region.

Finally, let us note that if the triplet zero-mode itself is light and is included in the light-scale theory, error estimates become more difficult. In this case, we also have to consider omitted operators of the Σ field. For present purposes, we shall be content with the rough estimate provided above for the heavy Σ case, and leave a more comprehensive analysis of the dimension-six operators for a future study.

6 Single-step transition in the ΣSM: results

We shall now assume that the triplet field is integrated out in the second step of DR and study the one-step scenario in this approximation. By performing DR as described above, we obtain a parameter mapping from the full ΣSM to the simplified 3d theory introduced in section 3.5. Nature of the EWPT and its critical temperature can be studied non-perturbatively by looking at the parameters $x \equiv \bar{\lambda}_3/\bar{g}_3^2$ and $y \equiv \bar{\mu}_{\phi,3}^2/\bar{g}_3^4$, evaluated at RG scale $\bar{\Lambda}_3 = \bar{g}_3^2$. Since these are now functions of the ΣSM parameters M_Σ, a_2 and b_4, we proceed to scan the parameter space spanned by M_Σ, a_2, b_4 and evaluate x and y at each point using the DR mapping. Temperature is then varied from 80 GeV to 200 GeV in steps of 10 GeV and the critical temperature T_c is determined by looking for solutions to $y(T) = 0$ using linear interpolation. At points with $y = 0$, the type of the transition is then determined by the value of x. Our scans reveal a region in the heavy Σ domain where $0 < x < 0.11$, indicating a first-order phase transition. In particular, we are able to accurately find the endpoints at which the first-order transition turns into a crossover, characterized by $x > 0.11$. This is not possible with purely perturbative methods.

Results of the parameter space scans have previously been published in the main paper [53]. Here we present additional plots that provide insight into inner workings of DR.

6.1 Main results and physical implications

Fig. 5 shows regions of first-order phase transition in (M_Σ, a_2) and (M_Σ, b_4) planes, scanned uniformly in steps of 5 GeV for M_Σ and 0.05 for a_2, b_4. The plots have been produced using full $O(g^4)$ DR for couplings and scalar masses, including the loop corrections to $\overline{\text{MS}}$ parameters, but Debye masses have been matched using $O(g^2)$ relations. The gray area corresponds to $\mu_\Sigma > 0$ where a two-step transition becomes possible. To quantitatively describe the EWPT in this region, the triplet needs to be dynamically included in the Monte Carlo simulations and therefore we make no statement about the phase transition there.

Curves of constant Δ_6, defined in Eq. (5.48), are illustrated in Figs. 5a and 5b to address credibility of the results. First-order transitions are found in a region where the above analysis of dimension-six operators estimates an error of roughly 10%. As the error grows larger, construction of the effective theory breaks down due to neglected higher-order operators in the dark-green region. Fig. 5b indicates that the transition bears reduced sensitivity to the triplet self coupling b_4. This is to be expected, since in the single-step scenario, transition dynamics are modified mainly by interactions of Σ with the Higgs field.

A first-order transition requires the remaining two parameters be sufficiently large, and we obtain lower bounds of $M_\Sigma \gtrsim 200$ GeV and $a_2 \gtrsim 1.5$. The reason for this becomes clear if one considers the effective theory used to study the transition: In the SM, the EWPT is a smooth crossover, with the x parameter becoming larger as the physical Higgs mass is increased. For m_H fixed at 125 GeV, large thermal corrections and therefore large couplings are needed to strengthen the transition enough to bring x sufficiently close to zero for a first-order transition to be possible. This raises concerns whether the perturbative construction of DR mappings is reliable in the region of interest. This question has been
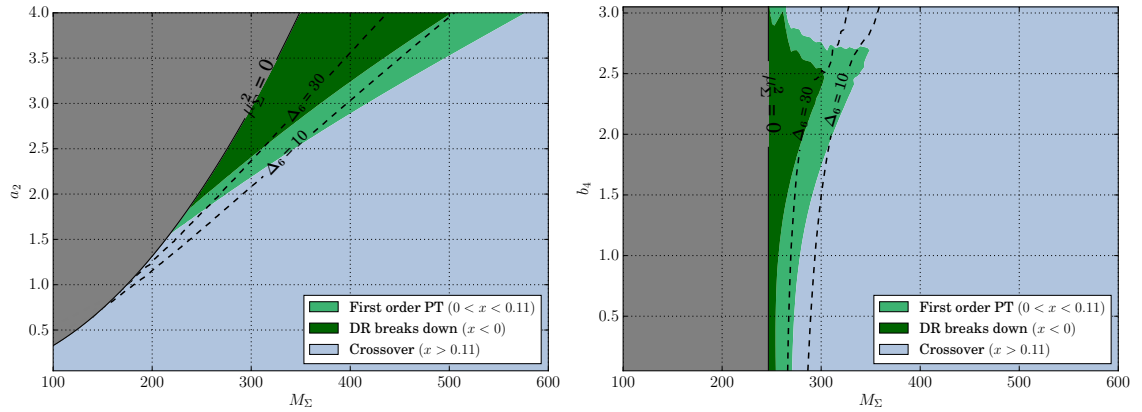
(a) Fixed $b_4 = 0.75$. A single-step transition favors large portal coupling a_2.

(b) Fixed $a_2 = 2.0$. The transition is relatively insensitive to the self-coupling b_4.
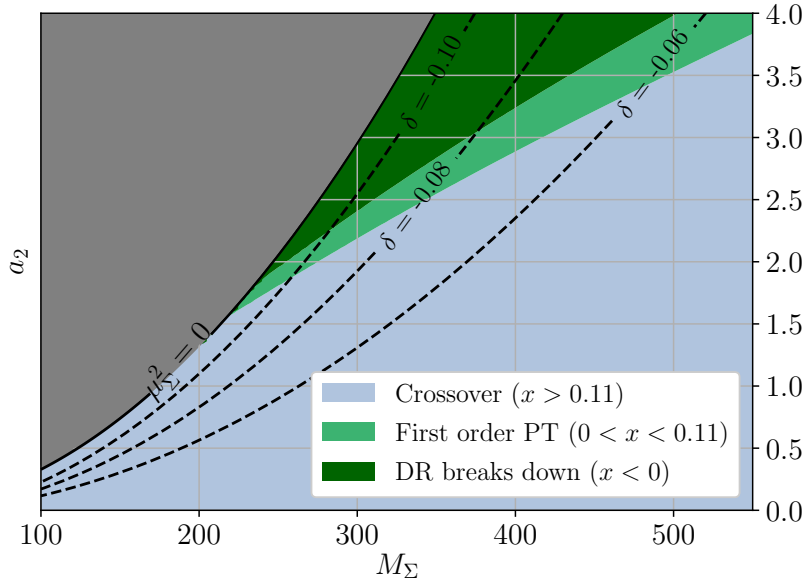
(c) Contour plot showing the relative shift caused to the SM value of $H \to \gamma\gamma$ decay width. We find first-order transitions in the negative-δ region, which is also slightly preferred by experiments [73].

Figure 5: Main results of our effective theory approach in the single-step transition region. Plots (a) and (c) have been published in the main paper [53].

addressed in Refs. [87, 88], where the authors conclude that the high-T expansion used in DR works well even if couplings are allowed to become large. We hope that forthcoming simulations on a dynamical triplet model will bring new insight on both the validity of DR, as well as that of perturbative studies of the EWPT performed in the full 4d theory.

A connection to collider phenomenology is provided by Fig. 5c. Parameter δ is defined
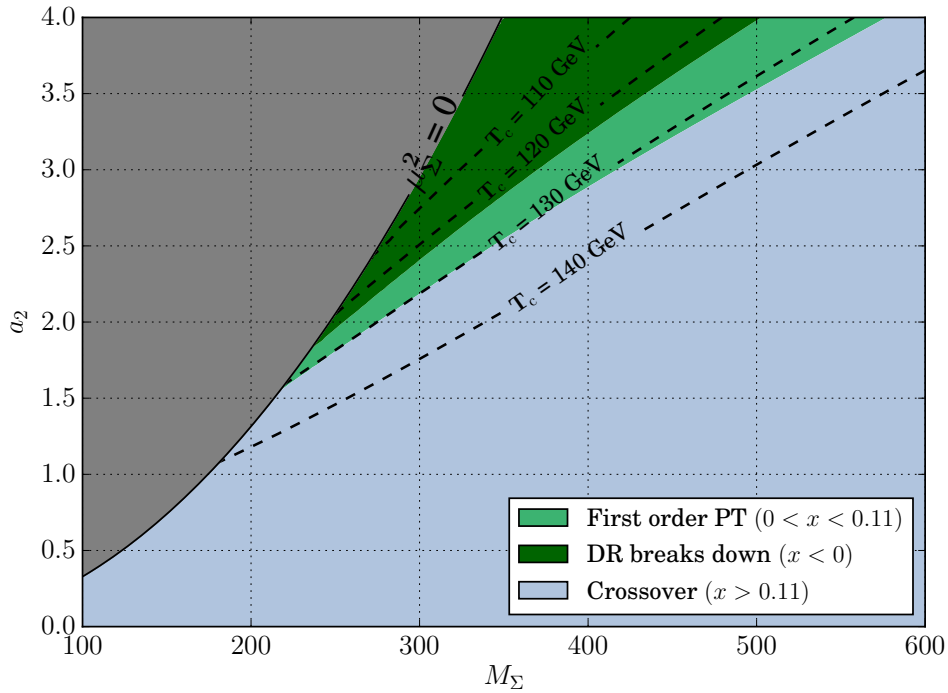
Figure 6: Critical temperature curves in the single-step transition region. A similar plot can be found in Ref. [53].

as the change in the Higgs-diphoton partial width relative to its SM value [52, 53],

$$\delta = \frac{\Gamma^{\Sigma\text{SM}}(h \to \gamma\gamma) - \Gamma^{\text{SM}}(h \to \gamma\gamma)}{\Gamma^{\text{SM}}(h \to \gamma\gamma)}. \tag{6.1}$$

Our analysis sees no first-order transitions in the light Σ region where δ is strongly constrained by experiments [73]. Conversely, deviations of $\sim 10\%$ when $M_\Sigma \gtrsim 200$ GeV are within current experimental bounds. Fig. 5c demonstrates that the requirement of a first-order transition sets a lower bound on the deviation $|\delta|$ for a given M_Σ. Future measurements on the decay rate may thus be used to probe the validity of the model.

Contours of critical temperature are shown in Fig. 6. Our analysis predicts a first-order transition in temperature range of $120 - 130$ GeV. Values of both the physical triplet mass M_Σ as well as the mass parameter μ_Σ are well below the thermal scale πT, justifying the inclusion of the triplet field in the heavy-scale 3d theory. Note that the curves of constant T_c closely follow x-contours, which determine the strength of the EWPT. The criterion for a transition strong enough for baryogenesis and graviational waves is roughly $x \gtrsim 0.04$, as demonstrated by the lattice analysis of Ref. [36]. Fig. 6 suggests that the transition strength is inversely proportional to T_c, which is in concordance with perturbative results [52].

6.2   Importance of the vacuum renormalization procedure

It is interesting to see how the results change if we omit loop corrections to the mass eigenvalues and match the $\overline{\text{MS}}$ parameters to physical quantities using only the tree-level relations given in Eqs. (5.27)-(5.32). This modifies the initial conditions of our DR mapping. Following the scanning protocol described above, this approximation leads to Fig. 7. Critical temperature in the white region is too large for realistic EWPT, $T_c > 200$ GeV, so we have not included it in our scans.
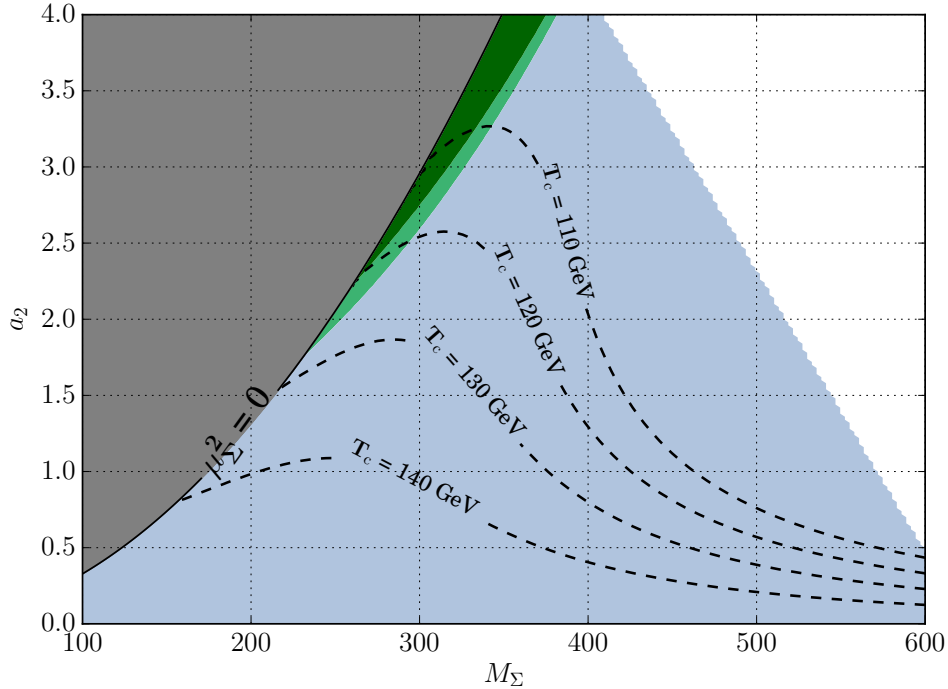
Figure 7: Regions of first-order phase transition and the respective T_c curves in the simplified case where tree-level eigenvalue relations have been used for the parameters. Errors in both T_c and x are significant in the large M_Σ limit.

The most obvious change from the proper loop-corrected plot in Fig. 6 is the behavior of T_c contours, which suffer from large deviations in the heavy M_Σ region. This is unfortunate, as knowledge of the critical temperature is crucial for gravitational-wave or baryon number predictions. Neglecting the initial loop corrections also cause considerable shrinking of the first-order region. We conclude that $O(g^4)$ corrections to $\overline{\text{MS}}$ parameters are indispensable in order to reliably study the EWPT via DR, at least if the BSM parameters are allowed to obtain large values.

6.3   One-loop approximation

Finally, let us consider omitting $O(g^4)$ corrections to mass parameter matching relations in both steps of DR. The two-loop calculation of scalar self-energies is often the most involved
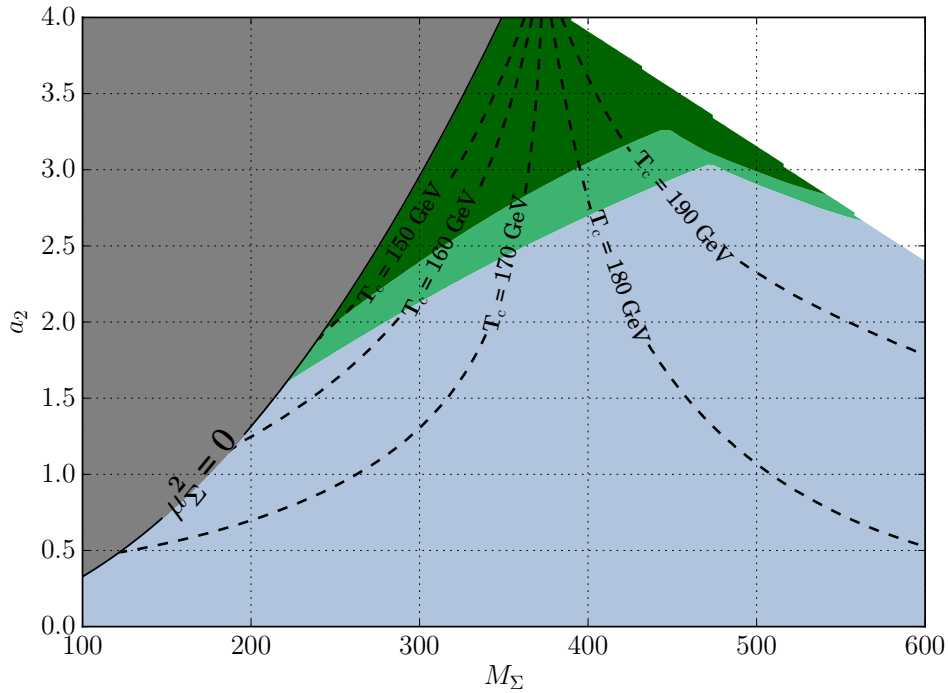
Figure 8: Results of parameter space scanning using one-loop matching for the scalar mass parameters. Input parameters have been evaluated at RG scale $\Lambda = 4\pi e^{-\gamma}$ using β functions. This approximation highly overestimates the critical temperature.

stage of the DR procedure, and it would be convenient to skip this computation if a one-loop matching is able to provide sufficient accuracy. Unfortunately, $O(g^2)$ mass parameter matching is unreliable already on theoretical grounds, as the resulting bare 3d mass is then explicitly dependent on the 4d RG scale Λ, and a similar problem arises in the second DR step. One may attempt to minimize the logarithmic running effects by performing the analysis at scale $\Lambda = 4\pi e^{-\gamma}$, which sets all one-loop logarithms to zero in the 4d theory.

The results in this approximation are illustrated in Fig. 8, with fixed $b_4 = 0.75$ as before. The first-order transition region becomes distorted at large M_Σ and a_2 due to running of 4d parameters that is not properly canceled from the mass parameter matching relations at one-loop level. Furthermore, relative errors in critical temperatures in the first-order region compared to the more accurate Fig. 6 are large, almost fifty percent at the worst. This behavior is unsurprising, as the critical temperature is directly related to the thermal correction of the doublet mass parameter. Corrections to the triplet mass also propagate to the final theory and can have considerable effect on the y parameter, especially. Thus, two-loop mass parameter matching should not be neglected in DR for quantitative results.

7 Summary

Electroweak baryogenesis is a promising candidate for explaining the origin of the baryon asymmetry in the present universe during the electroweak phase transition. It relies on sphaleron transitions that convert CP violation into baryon asymmetry during the bubble nucleation stage of the transition, provided that the phase transition is of strongly first order. However, new physics is required, as this transition in the Standard Model is a smooth crossover. By introducing new scalar fields, it is possible to strengthen the transition and make it first order, rendering electroweak baryogenesis a viable scenario in these extended models.

Independently of the question of baryogenesis, the full structure of the scalar sector remains an active area of both theoretical and experimental research. New scalars modify the phase transition dynamics via their couplings to the SM particles, which can leave observable signatures in branching ratios that can potentially be measured in collider experiments. Furthermore, first-order phase transitions are expected to produce gravitational-wave signals that could be detected in future detectors. Research of the electroweak baryogenesis is thus strongly coupled to the phenomenology of BSM theories and can provide insight into the viability of such models.

In this thesis, we have discussed effective theories that can be used to facilitate the study of the electroweak phase transition. These theories are three dimensional and are constructed by matching of static Green's functions. The effective theories have a universal structure, determined by the renormalization procedure that is essential for the parameter mapping. Although the matching procedure is perturbative, construction of the effective theories is free of infrared problems that otherwise render high-temperature perturbative calculations unreliable. Dimensional reduction bypasses these complications by implementing a resummation process that takes advantage of a thermal scale hierarchy generated by the heat bath. For this reason, dimensionally-reduced theories are, in many cases, preferred for EWPT analyses over the traditional effective potential approach in four dimensions. Of particular importance are non-perturbative lattice simulations that are readily performed on the effective theories.

We have applied dimensional reduction to the Standard Model augmented with a real triplet scalar. By treating the triplet as a sufficiently heavy field, it becomes justified to integrate it out, resulting in a light-scale theory identical to that obtained from the minimal SM. Using existing lattice results for this theory, we have performed a scan over the triplet model parameter space, identifying regions of a first-order phase transition and the corresponding critical temperatures in the domain where transition dynamics are not largely modified by the presence of the triplet. Such single-step transitions necessitate large values for the Higgs-triplet portal coupling, which may cause large uncertainties in the perturbative construction of the effective theory. However, this concern is present in many other extensions of the SM as well, and lattice simulations are needed to verify perturbative results obtained in these models. Starting by simulating the triplet dynamically on the lattice in the near future, our hope is to provide a trustworthy benchmark for the accuracy of perturbative calculations concerning the electroweak phase transition.

A Symmetric phase Feynman rules for the real triplet

We list Feynman rules for new vertices appearing in the ΣSM, with the theory being as defined in section 4.1. Rules for SM vertices in a similar setting have been presented in Ref. [61].

Scalar propagators:

$$j \ \text{--}\blacktriangleleft\text{--} \ i = \delta^{ij} \frac{1}{P^2 + (-\mu_\phi^2) + \delta_{P_0}\bar{\Pi}_\phi}, \tag{A.1}$$

$$a \ \text{=====} \ b = \delta^{ab} \frac{1}{P^2 + (-\mu_\Sigma^2) + \delta_{P_0}\bar{\Pi}_\Sigma}, \tag{A.2}$$

where $\delta_{P_0} \equiv \delta_{P_0,0}$, and $\bar{\Pi}$ are the thermal masses needed for resummation and are applied only for the $n = 0$ modes. The sign in front of the mass parameters follows from our sign convention in defining the scalar potential.

Interactions with the SU(2) gauge field:

$$= ig\epsilon^{abc}(K - P)_\mu \qquad\qquad = g^2(\delta^{ac}\delta^{bd} + \delta^{ad}\delta^{bc} - 2\delta^{ab}\delta^{cd})\delta_{\mu\nu} \tag{A.3}$$

Scalar interactions:

$$= -2b_4(\delta^{ac}\delta^{bd} + \delta^{ad}\delta^{bc} + \delta^{ab}\delta^{cd}) \qquad\qquad = -a_2\delta^{ij}\delta_{ab}. \tag{A.4}$$

For unoriented lines, the momenta are understood to flow into the vertex.

Counterterms and the thermal counterterm as defined in sections 5.1 and 5.4:

$$a \ \text{==}\blacksquare\text{==} \ b = -\delta_{ab}\left(P^2\delta Z_\Sigma - \delta\mu_\Sigma^2\right), \qquad a \ \text{==}\blacklozenge\text{==} \ b = \delta_{ab}\bar{\Pi}_\Sigma. \tag{A.5}$$

$$= \left(2g\delta g + g^2(\delta Z_A + \delta Z_\Sigma)\right)(\delta^{ac}\delta^{bd} + \delta^{ad}\delta^{bc} - 2\delta^{ab}\delta^{cd})\delta_{\mu\nu}$$

44

$$= -2\delta b_4(\delta^{ac}\delta^{bd} + \delta^{ad}\delta^{bc} + \delta^{ab}\delta^{cd}) \qquad = -\delta a_2 \delta^{ij}\delta_{ab}. \tag{A.6}$$

Rules for the heavy-scale 3d theory

Relevant propagators and vertex rules for the second step of DR are presented below. The theory is as defined in section 4.4.

Temporal scalar propagators:

$$
\begin{aligned}
\underline{\quad A_0 \quad} &= \delta^{ab}\frac{1}{p^2 + m_D^2}, \\
\underline{\quad B_0 \quad} &= \frac{1}{p^2 + m_D'^2}, \\
\underline{\quad C_0 \quad} &= \delta^{\alpha\beta}\frac{1}{p^2 + m_D''^2}.
\end{aligned}
\tag{A.7}
$$

Interaction vertices:

$$\frac{A_0^b}{\substack{k \\ p}}\!\!\!\bullet\!\!\sim ar = ig_3\epsilon^{abc}(k-p)_r, \qquad = g_3^2(\delta^{ac}\delta^{bd} + \delta^{ad}\delta^{bc} - 2\delta^{ab}\delta^{cd})\delta_{rs}, \tag{A.8}$$

$$= -2h_3\delta^{ab}\delta^{ij}, \qquad = -2h_3'\delta^{ij}, \qquad = -h_3''(\sigma_a)^{ij}, \tag{A.9}$$

$$= -2\omega_3\delta^{\alpha\beta}\delta^{ij}, \qquad = -4\delta_3\delta^{ab}\delta^{cd} - 2\delta_3'(\delta_{ac}\delta_{bd} + \delta_{ad}\delta_{bc}). \tag{A.10}$$

$$\tag{A.11}$$

Interactions with the 3d mass correction terms are given by

$$i \;\blacktriangleleft\!\blacklozenge\!\blacktriangleleft\!-\; j \;= \delta_{ij}\bar{\Pi}_{\phi,3}, \tag{A.12}$$

$$a \;=\!\!=\!\!\blacklozenge\!=\!\!=\; b \;= \delta_{ab}\bar{\Pi}_{\Sigma,3}. \tag{A.13}$$

B Diagrams for integration over the superheavy scale

Diagrams needed to construct the $O(g^4)$ DR mapping to the heavy-scale theory, calculated in the $\overline{\text{MS}}$ scheme, are listed in this appendix. It is assumed that the triplet field is either light or heavy. The results are written in terms of master integrals that have been defined and computed in Ref. [60]. For simplicity, the calculation is performed in Landau gauge; this reduces the number of needed diagrams drastically. Furthermore, we introduce the following short-hand notations to facilitate the calculation:

$$d = 3 - 2\epsilon, \tag{B.1}$$

$$N_c = 3 \quad \text{(number of quark colors)}, \tag{B.2}$$

$$N_f = 3 \quad \text{(number of fermion families)}, \tag{B.3}$$

$$N_d = 1 \quad \text{(contributions from the SU(2) doublet)}, \tag{B.4}$$
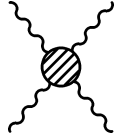
$$N_t = 1 \quad \text{(contributions from the SU(2) triplet)}. \tag{B.5}$$

Fermion hypercharges are given by $Y_\ell = -1, Y_e = -2, Y_q = \frac{1}{3}, Y_u = \frac{4}{3}, Y_d = -\frac{2}{3}$.

B.1 Four-point correlators
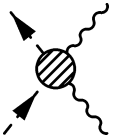
We list the one-loop corrections from superheavy fields to the relevant four-point correlation functions. These are needed for coupling constant matching relations.

The $A_0^a A_0^b A_0^c A_0^d$ correlator

$$= \frac{1}{6}(d-1)(d-3)\Big(8d - 8 + N_d + 8N_t + (1 - 2^{4-d})N_f(1 + N_c)\Big)$$
$$\times g^4(\delta_{ab}\delta_{cd} + \delta_{ac}\delta_{bd} + \delta_{ad}\delta_{bc})I_2^{4b}. \tag{B.6}$$

The $\phi_i^\dagger \phi_j A_\mu^a A_\nu^b$ correlator

$$= \delta_{ij}\delta_{ab}\Big\{d(d - \tfrac{25}{8})g^4 + \tfrac{d}{8}g^2 g'^2 + 3(d-3)\lambda g^2 + 2(d-3)a_2 g^2 \tag{B.7}$$

$$+ \tfrac{1}{2}(2^{4-d} - 1)(2 - d)g^2 N_c g_Y^2\Big\}I_2^{4b}$$
for $\mu = \nu = 0$,

$$\delta_{ij}\delta_{ab}\delta_{rs}\Big\{-\tfrac{3}{8}g^4 + \tfrac{3}{8}g^2 g'^2 - \tfrac{1}{2}(2^{4-d} - 1)g^2 N_c g_Y^2\Big\}I_2^{4b}$$
for $\mu = r$, $\nu = s$. \tag{B.8}

The $\Sigma^c \Sigma^d A_\mu^a A_\nu^b$ correlator

$$
= \left(2(3-d)g^2 b_4 + d(d-4)g^4\right)(\delta_{ac}\delta_{bd} + \delta_{ad}\delta_{bc})I_2^{4b}
$$

$$
+ \left((d-3)(8b_4 + a_2)g^2 + 2d(d-2)g^4\right)\delta_{ab}\delta_{cd}I_2^{4b} \tag{B.9}
$$

for $\mu = \nu = 0$,

$$
= -3g^4 \delta_{rs}(-2\delta_{ab}\delta_{cd} + \delta_{ac}\delta_{bd} + \delta_{ad}\delta_{bc})I_2^{4b} \tag{B.10}
$$

for $\mu = r$, $\nu = s$.

The $\phi_i^\dagger \phi_j \phi_k^\dagger \phi_\ell$ correlator

$$
= \left(24\lambda^2 + \frac{3}{2}a_2^2 + \frac{d}{8}(3g^4 + g'^4 + 2g^2 g'^2) - 2(2^{4-d} - 1)N_c g_{Y,n}^4\right)(\delta_{ik}\delta_{j\ell} + \delta_{i\ell}\delta_{jk})I_2^{4b}.
$$

$$
\tag{B.11}
$$

The $\phi_i^\dagger \phi_j \Sigma^a \Sigma^b$ correlator

$$
= \left(6a_2\lambda + 5a_2 b_4 + dg^4 + 2a_2^2\right)\delta_{ij}\delta_{ab}I_2^{4b}. \tag{B.12}
$$

The $\Sigma^a \Sigma^b \Sigma^c \Sigma^d$ correlator

$$
= \left(2a_2^2 + 22b_4^2 + 4dg^4\right)(\delta_{ab}\delta_{cd} + \delta_{ac}\delta_{bd} + \delta_{ad}\delta_{bc})I_2^{4b}. \tag{B.13}
$$

Correlators not listed here obtain no contributions from the triplet and have been calculated in Refs. [35, 61].

B.2 Two-point correlators

Again, we only list the superheavy contributions, needed for mass parameter and field matching.

SU(2)$_L$ gauge boson self-energy at one-loop

$a\mu$ $b\nu$

$$
\begin{aligned}
&= g^2\delta_{ab}\Big[-(d-1)(2d-2+N_d+2N_t)I_1^{4b} \\
&\quad + \tfrac{1}{6}\Big(-4(-5+N_d+2N_t)+d(N_d+2N_t-4+2d)\Big)P^2 I_2^{4b}\Big] \\
&\quad + g^2\delta_{ab}(d-1)N_f(1+N_c)\big[(2^{2-d}-1)I_1^{4b}-\tfrac{1}{6}(2^{4-d}-1)P^2 I_2^{4b}\big]
\end{aligned}
\tag{B.14}
$$
for $\mu=\nu=0$,

$$
= g^2\delta_{ab}\big[\tfrac{1}{6}(32-N_d-2N_t-2d)-\tfrac{1}{3}(2^{4-d}-1)N_f(1+N_c)\big](\delta_{rs}P^2-P_rP_s)I_2^{4b} \tag{B.15}
$$
for $\mu=r,\,\nu=s$.

P^2 is the external momentum, and its coefficient gives the 3d field normalization correction according to Eq. (3.8).

U(1)$_Y$ gauge boson self-energy at one-loop

μ ν

$$
\begin{aligned}
&= g'^2 N_d\big[(1-d)I_1^{4b}-\tfrac{2}{3}(1-\tfrac{d}{4})P^2 I_2^{4b}\big]-\tfrac{1}{2}g'^2(d-1)N_f \\
&\quad \times[2Y_\ell^2+Y_e^2+N_c(2Y_q^2+Y_u^2+Y_d^2)]\big[(1-2^{2-d})I_1^{4b}+\tfrac{1}{6}(2^{4-d}-1)P^2 I_2^{4b}\big]
\end{aligned}
\tag{B.16}
$$
for $\mu=\nu=0$,

$$
\begin{aligned}
&= -\tfrac{1}{6}g'^2\big\{N_d+(2^{4-d}-1)N_f[2Y_\ell^2+Y_e^2+N_c(2Y_q^2+Y_u^2+Y_d^2)]\big\} \\
&\quad \times (\delta_{rs}P^2-P_rP_s)I_2^{4b}
\end{aligned}
\tag{B.17}
$$
for $\mu=r,\,\nu=s$.

Gluons play an irrelevant role in the 3d theories, and loop corrections to temporal gluons are of higher order, so we omit writing down their correlators [61].

Scalar doublet ϕ self-energy
One-loop diagrams, evaluated at external momentum P:
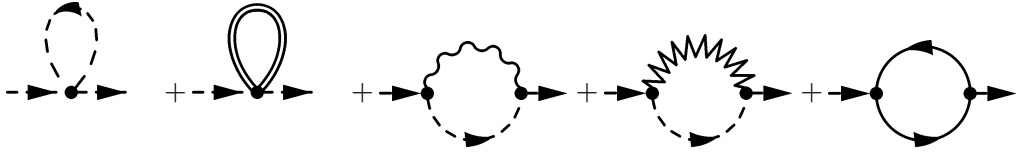
$$
\begin{aligned}
&= -6\lambda\delta_{ij}\Big(I_1^{4b}+\mu_\phi^2 I_2^{4b}\Big)-\frac{3}{2}a_2\delta_{ij}\Big(I_1^{4b}+\mu_\Sigma^2 I_2^{4b}\Big)-\frac{1}{4}d(3g^2+g'^2)\delta_{ij}I_1^{4b} \\
&\quad + 2(2^{2-d}-1)N_c y_t^2\delta_{ij}I_1^{4b}+\Big(\frac{9}{4}g^2+\frac{3}{4}g'^2-(2^{4-d}-1)N_c y_t^2\Big)\delta_{ij}P^2 I_2^{4b}.
\end{aligned}
\tag{B.18}
$$

The one-loop thermal mass correction $\bar{\Pi}_\phi$, needed for resummation, is obtained from the renormalized $P=0$ part. After including the tree-level mass counterterm diagram, one

obtains the $O(g^4)$ result

$$\bar{\Pi}_\phi \delta_{ij} = -\ i\ \blacktriangleleft\!\!-\!\!\oslash\!\!-\!\!\blacktriangleleft\text{-}\ j = \frac{T^2}{12}\left(6\lambda + \frac{3}{2}a_2 + \frac{3}{4}(3g^2 + g'^2) + N_c y_t^2\right)\delta_{ij}.$$

Two-loop fermionic diagrams:

$$(\text{B.19})$$

where

$$
\begin{aligned}
(a) &= \left(\frac{1}{2}g'^2 Y_q Y_u F_1(m'_D) + 8g_s^2 F_1(m''_D)\right)y_t^2 \delta_{ij},\\
(b) &= \left(\frac{3}{2}g^2 N_c F_2(m_D) + \frac{1}{2}g'^2 N_c(Y_q^2 + Y_u^2)F_2(m'_D) + 16g_s^2 F_2(m''_D)\right)y_t^2 \delta_{ij},\\
(c) &= \frac{N_f}{4}\delta_{ij}\left(3g^4(1 + N_c)F_3(m_D) + \frac{1}{2}g'^4\left(2Y_\ell^2 + Y_e^2 + N_c(2Y_q^2 + Y_u^2 + Y_d^2)\right)F_3(m'_D)\right),\\
(d) &= -6y_t^4 N_c \delta_{ij} F_4(\mu_\phi),\\
(e) &= -12N_c \lambda y_t^2 \delta_{ij} F_5(\mu_\phi).
\end{aligned}
$$

$$(\text{B.20})$$

49

Two-loop bosonic diagrams without the Σ field:

$$(\text{B.21})$$

where

$$(a) = 36\lambda^2 S_1(\mu_\phi, \mu_\phi)\delta_{ij},$$

$$(b) = \frac{3}{2}\lambda\left(3g^2 B_{11}(\mu_\phi, m_D) + g'^2 B_{11}(\mu_\phi, m'_D)\right)\delta_{ij},$$

$$(c) = \frac{1}{4}\left(3g^4 B_{12}(\mu_\phi, m_D) + g'^4 B_{12}(\mu_\phi, m'_D)\right)\delta_{ij},$$

$$(d) = -\frac{3}{4}g^4 B_2(m_D)\delta_{ij},$$

$$(e) = 12\lambda^2 S_3(\mu_\phi, \mu_\phi, \mu_\phi)\delta_{ij}, \qquad\qquad (\text{B.22})$$

$$(f) = \frac{1}{8}\left(3g^4 B_6(\mu_\phi, m_D, m_D) + g'^4 B_6(\mu_\phi, m'_D, m'_D) + 6g^2 g'^2 B_6(\mu_\phi, m_D, m'_D)\right)\delta_{ij},$$

$$(g) = -\frac{3}{2}\lambda\left(3g^2 B_4(\mu_\phi, m_D) + g'^2 B_4(\mu_\phi, m'_D)\right)\delta_{ij},$$

$$(h) = -3g^4 B_7(m_D)\delta_{ij},$$

$$(i) = -\frac{1}{8}\left(3g^4 B_5(\mu_\phi, m_D) + g'^4 B_5(\mu_\phi, m'_D)\right)\delta_{ij},$$

$$(j) = \frac{3}{2}g^4 B_3(m_D)\delta_{ij}.$$

Note that the 3d counterparts of diagrams (h) and (j) vanish in dimensional regularization due to exact cancellation of UV and IR divergences. When calculating the mass counterterm directly in the 3d theory, UV divergent contributions need to be explicitly extracted for the total counterterm to match that of the 4d theory.

Finally, two-loop contributions new in the ΣSM:

$$(B.23)$$

$$
\begin{aligned}
(a) &= 9\lambda a_2 \delta_{ij} S_1(\mu_\phi, \mu_\Sigma) + 3a_2^2 \delta_{ij} S_1(\mu_\Sigma, \mu_\phi) + \frac{15}{2} a_2 b_4 \delta_{ij} S_1(\mu_\Sigma, \mu_\Sigma), \\
(b) &= 3a_2 g^2 \delta_{ij} B_{11}(\mu_\Sigma, m_D) + \frac{3}{2} g^4 \delta_{ij} B_{12}(\mu_\Sigma, m_D), \\
(c) &= \frac{3}{2} a_2^2 \delta_{ij} S_3(\mu_\phi, \mu_\Sigma, \mu_\Sigma), \\
(d) &= -3a_2 g^2 \delta_{ij} B_4(\mu_\Sigma, m_D) - \frac{3}{4} g^4 \delta_{ij} B_5(\mu_\Sigma, m_D).
\end{aligned}
$$

$$(B.24)$$

One-loop counterterm diagrams:

$$(B.25)$$

where

$$(a) = 4N_c\Big(y_t\delta y_t + \frac{1}{2}y_t(\delta Z_\phi + \delta Z_q + \delta Z_t)\Big)\Big(2^{2-d} - 1\Big)\delta_{ij}I_1^{4b},$$

$$(b) = -2N_cy_t(\delta Z_q + \delta Z_t)\Big(2^{2-d} - 1\Big)\delta_{ij}I_1^{4b},$$

$$(c) = 6\lambda\delta Z_\phi\delta_{ij}I_1^{4b} - 6\delta\lambda\delta_{ij}I_1^{4b}$$

$$(d) = \frac{1}{4}\Big(3g^2\delta Z_A + g'^2\delta Z_B\Big)\delta_{ij}d\,I_1^{4b}, \tag{B.26}$$

$$(e) = -\frac{3}{4}\Big(2g\delta g + g^2(\delta Z_\phi + \delta Z_A)\Big)\delta_{ij}d\,I_1^{4b},$$

$$(f) = -\frac{1}{4}\Big(2g'\delta g' + g'^2(\delta Z_\phi + \delta Z_B)\Big)\delta_{ij}d\,I_1^{4b},$$

$$(g) = \frac{3}{2}a_2\delta_{ij}\delta Z_\Sigma I_1^{4b} - \frac{3}{2}\delta a_2\delta_{ij}I_1^{4b}\,.$$

Thermal counterterm diagrams that cancel terms linear in T from two-loop diagrams:

$$= -6\lambda\delta_{ij}\bar{\Pi}_\phi TI_2^3(\underline{\mu}_\phi) - \frac{3}{2}a_2\delta_{ij}\bar{\Pi}_\Sigma TI_2^3(\underline{\mu}_\Sigma) - \frac{3}{4}g^2\delta_{ij}m_D^2 TI_2^3(m_D) - \frac{1}{4}g'^2\delta_{ij}m_D'^2 TI_2^3(m_D').$$
$$\tag{B.27}$$

Scalar triplet Σ self-energy
One-loop diagrams, evaluated at external momentum P:
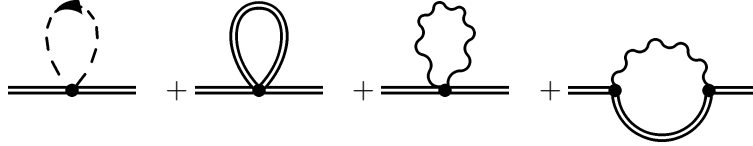
$$= -2a_2\delta_{ab}\Big(I_1^{4b} + \mu_\phi^2 I_2^{4b}\Big) - 5b_4\delta_{ab}\Big(I_1^{4b} + \mu_\Sigma^2 I_2^{4b}\Big) - 2g^2d\delta_{ab}I_1^{4b} + 6g^2P^2\delta_{ab}I_2^{4b}. \tag{B.28}$$

The $O(g^4)$ thermal mass correction is found to be

$$\bar{\Pi}_\Sigma = \frac{T^2}{12}(2a_2 + 5b_4 + 6g^2). \tag{B.29}$$

Two-loop diagrams:

$$\begin{aligned}
(a) &= 12\lambda a_2\delta_{ab}S_1(\mu_\phi,\mu_\phi) + 3a_2^2\delta_{ab}S_1(\mu_\phi,\mu_\Sigma) + 10b_4a_2\delta_{ab}S_1(\mu_\Sigma,\mu_\phi) \\
&\quad + 25b_4^2\delta_{ab}S_1(\mu_\Sigma,\mu_\Sigma), \\
(b) &= \frac{1}{2}a_2\delta_{ab}\Big(3g^2B_{11}(\mu_\phi,m_D) + g'^2B_{11}(\mu_\phi,m'_D)\Big), \\
(c) &= 10b_4g^2\delta_{ab}B_{11}(\mu_\Sigma,m_D) + 2g^4\delta_{ab}B_{12}(\mu_\phi,m_D) + 4g^4\delta_{ab}B_{12}(\mu_\Sigma,m_D), \\
(d) &= -2g^4\delta_{ab}B_2(m_D), \\
(e) &= 2a_2^2\delta_{ab}S_3(\mu_\phi,\mu_\phi,\mu_\Sigma) + 10b_4^2\delta_{ab}S_3(\mu_\Sigma,\mu_\Sigma,\mu_\Sigma) + 6g^4B_6(\mu_\Sigma,m_D,m_D), \\
(f) &= -10b_4g^2\delta_{ab}B_4(\mu_\Sigma,m_D) - \frac{1}{2}a_2\delta_{ab}\Big(3g^2B_4(\mu_\phi,m_D) + g'^2B_4(\mu_\phi,m'_D)\Big) \\
&\quad - 4a_2y_t^2N_c\delta_{ab}F_5(\mu_\phi), \\
(g) &= -2g^4\delta_{ab}B_5(\mu_\Sigma,m_D) - g^4\delta_{ab}B_5(\mu_\phi,m_D) + 2N_f(1+N_c)g^4\delta_{ab}F_3(m_D), \\
(h) &= -8g^4\delta_{ab}B_7(m_D) + 4g^4\delta_{ab}B_3(m_D).
\end{aligned}$$

(B.30)

(B.31)

One-loop counterterm diagrams:

$$(a)$$

$$(b)$$

$$(\text{B.32})$$

$$(a) = 2a_2\delta Z_\phi\delta_{ab}I_1^{4b} + 5b_4\delta Z_\Sigma\delta_{ab}I_1^{4b} - 2\delta a_2\delta_{ab}I_1^{4b} - 5\delta b_4\delta_{ab}I_1^{4b}$$

$$(b) = 2g^2 d\delta Z_A\delta_{ab}I_1^{4b} - 2\Big(2g\delta g + g^2(\delta Z_\Sigma + \delta Z_A)\Big)\delta_{ab}I_1^{4b} \qquad (\text{B.33})$$

Thermal resummation diagrams:

$$= 2a_2\delta_{ab}\bar\Pi_\phi T I_2^3(\underline{\mu}_\phi) + 5b_4\delta_{ab}\bar\Pi_\Sigma T I_2^3(\underline{\mu}_\Sigma) + 2g^2\delta_{ab}m_D^2 T I_2^3(m_D). \qquad (\text{B.34})$$
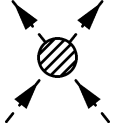
C Diagrams for integration over the heavy scale

Diagrams contributing to light-scale matching are presented here.

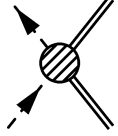## C.1 Integrating out temporal scalars A_0, B_0 and C_0

Here we assume that the triplet field is sufficiently light and can be included into the light-scale theory. We only list contributions from the temporal scalars, which are sufficient for parameter matching.

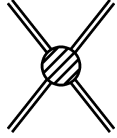**The $\phi_{i,3}^\dagger \phi_{j,3} \phi_{k,3}^\dagger \phi_{\ell,3}$ correlator**

$$= (\delta_{ij}\delta_{k\ell} + \delta_{i\ell}\delta_{jk})\big[6h_3^2 I_2^3(m_D) + 2h_3'^2 I_2^3(m_D') + h_3''^2 L_2^3(m_D, m_D')\big]. \tag{C.1}$$

The $\phi_{i,3}^\dagger \phi_{j,3} \Sigma_3^a \Sigma_3^b$ correlator

$$= 4h_3(3\delta_3 + \delta_3')\delta_{ij}\delta_{ab} I_2^3(m_D). \tag{C.2}$$

The $\Sigma_3^a \Sigma_3^b \Sigma_3^c \Sigma_3^d$ correlator

$$= 8(3\delta_3^2 + 2\delta_3\delta_3' + \delta_3'^{\,2})(\delta_{ab}\delta_{cd} + \delta_{ac}\delta_{bd} + \delta_{ad}\delta_{bc}) I_2^3(m_D). \tag{C.3}$$

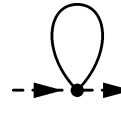**Gauge boson $A_{r,3}^a$ self-energy at one-loop**

$$ar \;\;\sim\!\!\!\bigcirc\!\!\!\sim\;\; bs = \frac{1}{3}g_3^2 \delta_{ab}(p_r p_s - \delta_{rs}p^2) I_2^3(m_D).$$

Scalar doublet ϕ_3 self-energy
At one-loop, there is the contribution

$$= -\big(3h_3 I_1^3(m_D) + h_3' I_1^3(m_D') + 8\omega_3 I_1^3(m_D'')\big)\delta_{ij}, \tag{C.4}$$

where the loop propagator is A_0, B_0 or C_0. This gives the one-loop mass correction analogously to the 4d thermal mass,

$$\bar{\Pi}_{\phi,3} = -\frac{1}{4\pi}(3h_3 m_D + h_3' m_D' + 8\omega_3 m_D''). \tag{C.5}$$

The correction is needed to cancel IR divergent terms of the form $1/\mu_{\phi,3}$ from two-loop diagrams.

Two-loop contributions and the 3d "resummation" diagrams:

$$(\mathrm{C.6})$$

where

$$
\begin{aligned}
(a) &= -6\lambda_3 \bar{\Pi}_{\phi_3} \delta_{ij} I_2^3(\underline{\mu}_{\phi,3}) - \frac{3}{2} a_{2,3} \bar{\Pi}_{\Sigma,3} \delta_{ij} I_2^3(\underline{\mu}_{\Sigma,3}), \\
(b) &= -6h_3 g_3^2 \delta_{ij} B_4^3(m_D, m_D) - \frac{3}{4} g_3^4 \delta_{ij} B_5^3(m_D, m_D), \\
(c) &= \delta_{ij}\Big(6h_3^2 S_3^3(\mu_{\phi,3}, m_D, m_D) + 2h_3'^{\,2} S_3^3(\mu_{\phi,3}, m_D', m_D') \\
&\quad + 3h_3''^{2} S_3^3(\mu_{\phi,3}, m_D, m_D')\Big), \\
(d) &= \delta_{ij}\Big(18\lambda_3 h_3 I_2^3(\mu_{\phi,3}) I_1^3(m_D) + 6\lambda_3 h_3' I_2^3(\mu_{\phi,3}) I_1^3(m_D')\Big), \\
(e) &= 3a_{2,3}(3\delta_3 + \delta_3')\delta_{ij} I_2^3(\mu_{\Sigma,3}) I_1^3(m_D), \\
(f) &= \delta_{ij}\Big(12h_3^2 I_1^3(\mu_{\phi,3}) I_2^3(m_D) + 4h_3'^{\,2} I_1^3(\mu_{\phi,3}) I_2^3(m_D')\Big), \\
(g) &= 6h_3(3\delta_3 + \delta_3')\delta_{ij} I_2^3(m_D) I_1^3(\mu_{\Sigma,3}).
\end{aligned}
$$

$$(\mathrm{C.7})$$

Note that two-loop contributions from the temporal gluons are of higher order.

Scalar triplet Σ_3 self-energy
One-loop:

$$ = -2(3\delta_3 + \delta_3')\delta_{ab} I_1^3(m_D), \qquad (\mathrm{C.8})$$

from which the mass correction is obtained as

$$\bar{\Pi}_{\Sigma,3} = -\frac{m_D}{2\pi}(3\delta_3 + \delta_3'). \qquad (\mathrm{C.9})$$

Two-loop and 3d resummation diagrams:

$$\tag{C.10}$$

where

$$
\begin{aligned}
(a) &= -2a_{2,3}\delta_{ab}\bar{\Pi}_{\phi,3}I_2^3(\underline{\mu}_{\phi,3}) - 5b_{4,3}\delta_{ab}\bar{\Pi}_{\Sigma,3}I_2^3(\underline{\mu}_{\Sigma,3}), \\
(b) &= 2a_{2,3}\Big(3h_3 I_1^3(m_D) + h_3' I_1^3(m_D')\Big)\delta_{ab}I_2^3(\mu_{\phi,3}), \\
(c) &= 10b_{4,3}(3\delta_3 + \delta_3')\delta_{ab}I_2^3(\mu_{\Sigma,3})I_1^3(m_D), \\
(d) &= 8h_3(3\delta_3 + \delta_3')\delta_{ab}I_2^3(m_D)I_1^3(\mu_{\phi,3}), \\
(e) &= 4(3\delta_3 + \delta_3')^2\delta_{ab}I_2^3(m_D)I_1^3(\mu_{\Sigma,3}), \\
(f) &= 8(3\delta_3^2 + 2\delta_3\delta_3' + 2\delta_3'^2)\delta_{ab}S_3^3(\mu_{\Sigma,3}, m_D, m_D), \\
(g) &= -4(3\delta_3 + \delta_3')g_3^2\delta_{ab}\,B_4^3(m_D) - 2g_3^4\delta_{ab}\,B_5^3(m_D).
\end{aligned}
\tag{C.11}
$$

C.2 Integrating out heavy Σ

Finally, we present a diagrammatic calculation for the heavy Σ case. In this scenario, the triplet field is integrated out together with the temporal scalars, and the relevant diagrams are listed here.

The $\phi_{i,3}^\dagger\phi_{j,3}\phi_{k,3}^\dagger\phi_{\ell,3}$ correlator

$$
= (\delta_{ij}\delta_{k\ell} + \delta_{i\ell}\delta_{jk})\left(\frac{1}{3}a_{2,3}^2 I_2^3(\mu_{\Sigma,3}) + 6h_3^2 I_2^3(m_D) + 2h_3'^2 I_2^3(m_D') + h_3''^2 L_2^3(m_D, m_D')\right).
\tag{C.12}
$$

Gauge boson $A_{r,3}^a$ self-energy at one-loop

$$
ar \;\sim\!\!\!\bigcirc\!\!\!\sim\; bs = \frac{1}{3}g_3^2\delta_{ab}(p_r p_s - \delta_{rs}p^2)\big(I_2^3(m_D) + I_2^3(\mu_{\Sigma,3})\big).
$$

Scalar doublet ϕ_3 self-energy

In addition to those listed in the previous section, there is the one-loop diagram

$$\text{[diagram]} = -\frac{3}{2}a_{2,3}\delta_{ij}I_1^3(\mu_{\Sigma,3}), \tag{C.13}$$

which modifies the mass correction:

$$\bar{\Pi}_{\phi,3} = -\frac{1}{4\pi}\left(\frac{3}{2}a_{2,3}\mu_{\Sigma,3} + 3h_3 m_D + h_3' m_D' + 8\omega_3 m_D''\right). \tag{C.14}$$

At two-loop level, new contributions are obtained from diagrams

$$\underbrace{\text{[diagram]}}_{(a)} + \underbrace{\text{[diagram]}}_{(b)} + \underbrace{\text{[diagram]}}_{(c)} + \underbrace{\text{[diagram]}\ +\ \text{[diagram]}}_{(d)}, \tag{C.15}$$

where

$$\begin{aligned}
(a) &= 9\lambda_3 a_{2,3}\delta_{ij}I_2^3(\mu_{\phi,3})I_1^3(\mu_{\Sigma,3}) + 3a_{2,3}^2\delta_{ij}I_2^3(\mu_{\Sigma,3})I_1^3(\mu_{\phi,3}),\\
(b) &= \frac{15}{2}a_{2,3}b_{4,3}\delta_{ij}I_2^3(\mu_{\Sigma,3})I_1^3(\mu_{\Sigma,3}),\\
(c) &= \frac{3}{2}a_{2,3}^2\delta_{ij}S_3^3(\mu_{\phi,3},\mu_{\Sigma,3},\mu_{\Sigma,3}),\\
(d) &= -3a_{2,3}g_3^2\delta_{ij}B_4^3(\mu_{\Sigma,3}) - \frac{3}{4}g_3^4\delta_{ij}B_5^3(\mu_{\Sigma,3}).
\end{aligned} \tag{C.16}$$

No mass corrections to the Σ field propagator are included in this case as the mass parameter $\mu_{\Sigma,3}$ is heavy, and therefore terms of the form $1/\mu_{\Sigma,3}$ are IR safe.

D   One-loop counterterms in the ΣSM

In this appendix, we list the $\overline{\text{MS}}$ counterterms required for $O(g^4)$ renormalization of the full theory. For definitions, see section 5.1. Although our diagrammatic calculation is performed in Landau gauge, we choose to express the counterterms in a general ξ gauge. This is useful for vacuum renormalization, necessary to obtain $O(g^4)$ corrections to the $\overline{\text{MS}}$ parameters, which is more convenient to perform in Feynman gauge (see section 5.5).

$$\delta Z_A = \frac{g^2}{16\pi^2\epsilon}\Big(\frac{26 - N_d - 2N_t}{6} - \frac{4}{3}N_f - \xi\Big), \tag{D.1}$$

$$\delta Z_B = -\frac{g'^2}{96\pi^2\epsilon}\Big(N_d + N_f\big[2Y_\ell^2 + Y_e^2 + 3(2Y_q^2 + Y_u^2 + Y_d^2)\big]\Big) = -\frac{g'^2}{96\pi^2\epsilon}\Big(N_d + \frac{40}{3}N_f\Big), \tag{D.2}$$

$$\delta Z_\phi = \frac{1}{16\pi^2\epsilon}\Big(\frac{3}{4}(3-\xi)g^2 + \frac{1}{4}(3-\xi)g'^2 - 3y_t^2\Big), \tag{D.3}$$

$$\delta Z_\Sigma = \frac{1}{16\pi^2\epsilon}\Big(2(3-\xi)g^2\Big), \tag{D.4}$$

$$\delta Z_q = -\frac{1}{16\pi^2\epsilon}\Big(\frac{1}{2}y_t^2 + \xi\big(\frac{3}{4}g^2 + \frac{1}{4}Y_q^2 g'^2 + \frac{4}{3}g_s^2\big)\Big), \tag{D.5}$$

$$\delta Z_t = -\frac{1}{16\pi^2\epsilon}\Big(y_t^2 + \xi\big(\frac{1}{4}Y_u^2 g'^2 + \frac{4}{3}g_s^2\big)\Big) \tag{D.6}$$

$$\delta Z_l = -\frac{1}{16\pi^2\epsilon}\frac{\xi}{4}\Big(3g^2 + Y_l^2 g'^2\Big), \tag{D.7}$$

$$\delta g = -\frac{g^3}{16\pi^2\epsilon}\Big(\frac{44 - N_d - 2N_t}{12} - \frac{2}{3}N_f\Big), \tag{D.8}$$

$$\delta g' = \frac{g'^3}{192\pi^2\epsilon}\Big(N_d + \frac{40}{3}N_f\Big), \tag{D.9}$$

$$\delta y_t = -\frac{y_t}{16\pi^2\epsilon}\Big(\frac{1}{3}g'^2 + 4g_s^2 + \xi\big(\frac{3}{4}g^2 + \frac{13}{36}g'^2 + \frac{4}{3}g_s^2\big)\Big). \tag{D.10}$$

Scalar counterterms:

$$\delta\mu_\phi^2 = \frac{1}{16\pi^2}\frac{1}{\epsilon}\Big(6\lambda\mu_\phi^2 + \frac{3}{2}a_2\mu_\Sigma^2 - \frac{1}{4}\xi\mu_\phi^2(3g^2 + g'^2)\Big), \tag{D.11}$$

$$\delta\mu_\Sigma^2 = \frac{1}{16\pi^2}\frac{1}{\epsilon}\Big(2a_2\mu_\phi^2 + 5b_4\mu_\Sigma^2 - 2\xi g^2\mu_\Sigma^2\Big), \tag{D.12}$$

$$\delta\lambda = \frac{1}{16\pi^2}\frac{1}{\epsilon}\frac{1}{2}\Big(24\lambda^2 + \frac{3}{2}a_2^2 + \frac{3}{8}(3g^4 + g'^4 + 2g^2g'^2) - 6y_t^4 - \xi\lambda(3g^2 + g'^2)\Big), \tag{D.13}$$

$$\delta a_2 = \frac{1}{16\pi^2}\frac{1}{\epsilon}\Big(2a_2^2 + 5a_2 b_4 + 3g^4 + 6a_2\lambda - \frac{1}{4}\xi a_2(11g^2 + g'^2)\Big), \tag{D.14}$$

$$\delta b_4 = \frac{1}{16\pi^2}\frac{1}{\epsilon}\Big(a_2^2 + 11b_4^2 + 6g^4 - 4\xi g^2 b_4\Big). \tag{D.15}$$

References

[1] P. A. R. Ade et al. Planck 2015 results. XIII. Cosmological parameters. *Astron. Astrophys.*, 594:A13, 2016.

[2] P. B. Arnold and L. D. McLerran. Sphalerons, Small Fluctuations and Baryon Number Violation in Electroweak Theory. *Phys. Rev.*, D36:581, 1987.

[3] A. D. Sakharov. Violation of CP Invariance, c Asymmetry, and Baryon Asymmetry of the Universe. *Pisma Zh. Eksp. Teor. Fiz.*, 5:32–35, 1967. [Usp. Fiz. Nauk161,61(1991)].

[4] A. Riotto. Theories of baryogenesis. In *Proceedings, Summer School in High-energy physics and cosmology: Trieste, Italy, June 29-July 17, 1998*, pages 326–436, 1998.

[5] A. D. Dolgov. Baryogenesis, 30 years after. In *Surveys in high-energy physics. Proceedings, 25th ITEP Winter School, Snegiri, Russia, February, 1997*, 1997.

[6] J. M. Cline. Baryogenesis. In *Les Houches Summer School - Session 86: Particle Physics and Cosmology: The Fabric of Spacetime Les Houches, France, July 31-August 25, 2006*, 2006.

[7] E. W. Kolb and M. S. Turner. The Early Universe. *Front. Phys.*, 69:1–547, 1990.

[8] A. G. Cohen, D. B. Kaplan, and A. E. Nelson. Progress in electroweak baryogenesis. *Ann. Rev. Nucl. Part. Sci.*, 43:27–70, 1993.

[9] M. Trodden. Electroweak baryogenesis. *Rev. Mod. Phys.*, 71:1463–1500, 1999.

[10] V. A. Rubakov and M. E. Shaposhnikov. Electroweak baryon number nonconservation in the early universe and in high-energy collisions. *Usp. Fiz. Nauk*, 166:493–537, 1996. [Phys. Usp.39,461(1996)].

[11] A. Riotto and M. Trodden. Recent progress in baryogenesis. *Ann. Rev. Nucl. Part. Sci.*, 49:35–75, 1999.

[12] M. Quiros. Finite temperature field theory and phase transitions. In *Proceedings, Summer School in High-energy physics and cosmology: Trieste, Italy, June 29-July 17, 1998*, pages 187–259, 1999.

[13] M. Dine and A. Kusenko. The Origin of the matter - antimatter asymmetry. *Rev. Mod. Phys.*, 76:1, 2003.

[14] D. E. Morrissey and M. J. Ramsey-Musolf. Electroweak baryogenesis. *New J. Phys.*, 14:125003, 2012.

[15] G. A. White. *A Pedagogical Introduction to Electroweak Baryogenesis*. IOP Concise Physics. Morgan & Claypool, 2016.

[16] S. Weinberg. Gauge and Global Symmetries at High Temperature. *Phys. Rev.*, D9:3357–3378, 1974.

[17] D. A. Kirzhnits. Weinberg model in the hot universe. *JETP Lett.*, 15:529–531, 1972. [Pisma Zh. Eksp. Teor. Fiz.15,745(1972)].

[18] D. A. Kirzhnits and A. D. Linde. Macroscopic Consequences of the Weinberg Model. *Phys. Lett.*, 42B:471–474, 1972.

[19] D. A. Kirzhnits and A. D. Linde. Symmetry Behavior in Gauge Theories. *Annals Phys.*, 101:195–238, 1976.

[20] S. L. Adler. Axial vector vertex in spinor electrodynamics. *Phys. Rev.*, 177:2426–2438, 1969.

[21] F. R. Klinkhamer and N. S. Manton. A Saddle Point Solution in the Weinberg-Salam Theory. *Phys. Rev.*, D30:2212, 1984.

[22] V. A. Kuzmin, V. A. Rubakov, and M. E. Shaposhnikov. On the Anomalous Electroweak Baryon Number Nonconservation in the Early Universe. *Phys. Lett.*, 155B:36, 1985.

[23] M. E. Shaposhnikov. Baryon Asymmetry of the Universe in Standard Electroweak Theory. *Nucl. Phys.*, B287:757–775, 1987.

[24] M. E. Shaposhnikov. Structure of the High Temperature Gauge Ground State and Electroweak Production of the Baryon Asymmetry. *Nucl. Phys.*, B299:797–817, 1988.

[25] G. R. Farrar and M. E. Shaposhnikov. Baryon asymmetry of the universe in the standard electroweak theory. *Phys. Rev.*, D50:774, 1994.

[26] G. R. Farrar and M. E. Shaposhnikov. Baryon asymmetry of the universe in the minimal Standard Model. *Phys. Rev. Lett.*, 70:2833–2836, 1993. [Erratum: Phys. Rev. Lett.71,210(1993)].

[27] M. E. Shaposhnikov. Possible Appearance of the Baryon Asymmetry of the Universe in an Electroweak Theory. *JETP Lett.*, 44:465–468, 1986. [Pisma Zh. Eksp. Teor. Fiz.44,364(1986)].

[28] C. Caprini et al. Science with the space-based interferometer eLISA. II: Gravitational waves from cosmological phase transitions. *JCAP*, 1604(04):001, 2016.

[29] D. J. Weir. Gravitational waves from a first order electroweak phase transition: a brief review. *Phil. Trans. Roy. Soc. Lond.*, A376:20170126, 2018.

[30] M. Hindmarsh, S. J. Huber, K. Rummukainen, and D. J. Weir. Shape of the acoustic gravitational wave power spectrum from a first order phase transition. *Phys. Rev.*, D96(10):103520, 2017.

[31] A. D. Linde. Infrared Problem in Thermodynamics of the Yang-Mills Gas. *Phys. Lett.*, 96B:289–292, 1980.

[32] D. J. Gross, R. D. Pisarski, and L. G. Yaffe. QCD and Instantons at Finite Temperature. *Rev. Mod. Phys.*, 53:43, 1981.

[33] P. de Forcrand. Simulating QCD at finite density. *PoS*, LAT2009:010, 2009.

[34] K. Farakos, K. Kajantie, K. Rummukainen, and M. E. Shaposhnikov. 3-D physics and the electroweak phase transition: Perturbation theory. *Nucl. Phys.*, B425:67–109, 1994.

[35] K. Kajantie, M. Laine, K. Rummukainen, and M. E. Shaposhnikov. Generic rules for high temperature dimensional reduction and their application to the standard model. *Nucl. Phys.*, B458:90–136, 1996.

[36] K. Kajantie, M. Laine, K. Rummukainen, and M. E. Shaposhnikov. The Electroweak phase transition: A Nonperturbative analysis. *Nucl. Phys.*, B466:189–258, 1996.

[37] K. Kajantie, M. Laine, K. Rummukainen, and M. E. Shaposhnikov. A Nonperturbative analysis of the finite T phase transition in SU(2) x U(1) electroweak theory. *Nucl. Phys.*, B493:413–438, 1997.

[38] K. Kajantie, M. Laine, K. Rummukainen, and M. E. Shaposhnikov. Is there a hot electroweak phase transition at m(H) larger or equal to m(W)? *Phys. Rev. Lett.*, 77:2887–2890, 1996.

[39] M. Gurtler, E.-M. Ilgenfritz, and A. Schiller. Where the electroweak phase transition ends. *Phys. Rev.*, D56:3888–3895, 1997.

[40] F. Csikor, Z. Fodor, and J. Heitger. Endpoint of the hot electroweak phase transition. *Phys. Rev. Lett.*, 82:21–24, 1999.

[41] M. B. Gavela, P. Hernandez, J. Orloff, and O. Pene. Standard model CP violation and baryon asymmetry. *Mod. Phys. Lett.*, A9:795–810, 1994.

[42] P. Huet and E. Sather. Electroweak baryogenesis and standard model CP violation. *Phys. Rev.*, D51:379–394, 1995.

[43] M. B. Gavela, P. Hernandez, J. Orloff, O. Pene, and C. Quimbay. Standard model CP violation and baryon asymmetry. Part 2: Finite temperature. *Nucl. Phys.*, B430:382–426, 1994.

[44] M. E. Carrington. The Effective potential at finite temperature in the Standard Model. *Phys. Rev.*, D45:2933–2944, 1992.

[45] W. Buchmuller, P. Di Bari, and M. Plumacher. Leptogenesis for pedestrians. *Annals Phys.*, 315:305–351, 2005.

[46] A. Pilaftsis and T. E. J. Underwood. Resonant leptogenesis. *Nucl. Phys.*, B692:303–345, 2004.

[47] J. M. Cline. Is electroweak baryogenesis dead? In *Proceedings, 52nd Rencontres de Moriond on Electroweak Interactions and Unified Theories: La Thuile, Italy, March 18-25, 2017*, 2017.

[48] L. Dolan and R. Jackiw. Gauge Invariant Signal for Gauge Symmetry Breaking. *Phys. Rev.*, D9:2904, 1974.

[49] N. K. Nielsen. On the Gauge Dependence of Spontaneous Symmetry Breaking in Gauge Theories. *Nucl. Phys.*, B101:173–188, 1975.

[50] M. Laine. Gauge dependence of the high temperature two loop effective potential for the Higgs field. *Phys. Rev.*, D51:4525–4532, 1995.

[51] H. H. Patel and M. J. Ramsey-Musolf. Baryon Washout, Electroweak Phase Transition, and Perturbation Theory. *JHEP*, 07:029, 2011.

[52] H. H. Patel and M. J. Ramsey-Musolf. Stepping Into Electroweak Symmetry Breaking: Phase Transitions and Higgs Phenomenology. *Phys. Rev.*, D88:035013, 2013.

[53] L. Niemi, H. H. Patel, M. J. Ramsey-Musolf, T. V. I. Tenkanen, and D. J. Weir. Electroweak phase transition in the ΣSM - I: Dimensional reduction. 2018.

[54] M. Laine. Effective theories of MSSM at high temperature. *Nucl. Phys.*, B481:43–84, 1996. [Erratum: Nucl. Phys.B548,637(1999)].

[55] M. Laine and K. Rummukainen. Two Higgs doublet dynamics at the electroweak phase transition: A Nonperturbative study. *Nucl. Phys.*, B597:23–69, 2001.

[56] M. Losada. The Two loop finite temperature effective potential of the MSSM and baryogenesis. *Nucl. Phys.*, B537:3–31, 1999.

[57] M. Losada. High temperature dimensional reduction of the MSSM and other multiscalar models. *Phys. Rev.*, D56:2893–2913, 1997.

[58] J. O. Andersen. Dimensional reduction of the two Higgs doublet model at high temperature. *Eur. Phys. J.*, C11:563–570, 1999.

[59] J. O. Andersen, T. Gorda, A. Helset, L. Niemi, T. V. I. Tenkanen, A. Tranberg, A. Vuorinen, and D. J. Weir. On the nature of the electroweak phase transition in the two Higgs doublet model. 2017.

[60] T. Gorda, A. Helset, L. Niemi, T. V. I. Tenkanen, and D. J. Weir. Electroweak phase transition and dimensional reduction of the Two-Higgs-Doublet Model. 2018.

[61] T. Brauner, T. V. I. Tenkanen, A. Tranberg, A. Vuorinen, and D. J. Weir. Dimensional reduction of the Standard Model coupled to a new singlet scalar field. *JHEP*, 03:007, 2017.

[62] J. I. Kapusta and C. Gale. *Finite-temperature field theory: Principles and applications.* Cambridge University Press, 2011.

[63] M. Laine and A. Vuorinen. Basics of Thermal Field Theory. *Lect. Notes Phys.*, 925:pp.1–281, 2016.

[64] R. D. Pisarski. Scattering Amplitudes in Hot Gauge Theories. *Phys. Rev. Lett.*, 63:1129, 1989.

[65] E. Braaten and R. D. Pisarski. Soft Amplitudes in Hot Gauge Theories: A General Analysis. *Nucl. Phys.*, B337:569–634, 1990.

[66] P. H. Ginsparg. First Order and Second Order Phase Transitions in Gauge Theories at Finite Temperature. *Nucl. Phys.*, B170:388–408, 1980.

[67] T. Appelquist and R. D. Pisarski. High-Temperature Yang-Mills Theories and Three-Dimensional Quantum Chromodynamics. *Phys. Rev.*, D23:2305, 1981.

[68] A. Jakovac. Reduction of the n component scalar model at two loop level. *Phys. Rev.*, D53:4538–4551, 1996.

[69] C. P. Burgess. Introduction to Effective Field Theory. *Ann. Rev. Nucl. Part. Sci.*, 57:329–362, 2007.

[70] K. Farakos, K. Kajantie, K. Rummukainen, and M. E. Shaposhnikov. 3-d physics and the electroweak phase transition: A Framework for lattice Monte Carlo analysis. *Nucl. Phys.*, B442:317–363, 1995.

[71] A. Katz and M. Perelstein. Higgs Couplings and Electroweak Phase Transition. *JHEP*, 07:108, 2014.

[72] A. Katz, M. Perelstein, M. J. Ramsey-Musolf, and P. Winslow. Stop-Catalyzed Baryogenesis Beyond the MSSM. *Phys. Rev.*, D92(9):095019, 2015.

[73] P. Fileviez Perez, H. H. Patel, M. Ramsey-Musolf, and K. Wang. Triplet Scalars and Dark Matter at the LHC. *Phys. Rev.*, D79:055024, 2009.

[74] M. Cirelli, A. Strumia, and M. Tamburini. Cosmology and Astrophysics of Minimal Dark Matter. *Nucl. Phys.*, B787:152–175, 2007.

[75] J. F. Gunion, R. Vega, and J. Wudka. Higgs triplets in the standard model. *Phys. Rev.*, D42:1673–1691, 1990.

[76] J. F. Gunion, H. E. Haber, G. L. Kane, and S. Dawson. The Higgs Hunter's Guide. *Front. Phys.*, 80:1–404, 2000.

[77] J. Brandstetter. Higgs boson results on couplings to fermions, CP parameters and perspectives for HL-LHC (ATLAS AND CMS). In *International Workshop on Future Linear Collider (LCWS2017) Strasbourg, France, October 23-27, 2017*, 2018.

[78] G. Aad et al. Search for charginos nearly mass degenerate with the lightest neutralino based on a disappearing-track signature in pp collisions at $\sqrt{(s)}$=8 TeV with the ATLAS detector. *Phys. Rev.*, D88(11):112006, 2013.

[79] V. Khachatryan et al. Search for disappearing tracks in proton-proton collisions at $\sqrt{s} = 8$ TeV. *JHEP*, 01:096, 2015.

[80] S. Inoue, G. Ovanesyan, and M. J. Ramsey-Musolf. Two-Step Electroweak Baryogenesis. *Phys. Rev.*, D93:015013, 2016.

[81] A. Hammerschmitt, J. Kripfganz, and M. G. Schmidt. Baryon asymmetry from a two stage electroweak phase transition? *Z. Phys.*, C64:105–110, 1994.

[82] M. E. Shaposhnikov. Finite temperature effective theories. *Subnucl. Ser.*, 34:360–397, 1997.

[83] E. Braaten and A. Nieto. Effective field theory approach to high temperature thermodynamics. *Phys. Rev.*, D51:6990–7006, 1995.

[84] P. B. Arnold and O. Espinosa. The Effective potential and first order phase transitions: Beyond leading-order. *Phys. Rev.*, D47:3546, 1993. [Erratum: Phys. Rev.D50,6662(1994)].

[85] D. Bailin and A. Love. *INTRODUCTION TO GAUGE FIELD THEORY*. 1986.

[86] M. E. Peskin and D. V. Schroeder. *An Introduction to quantum field theory*. Addison-Wesley, Reading, USA, 1995.

[87] M. Laine and M. Losada. Two loop dimensional reduction and effective potential without temperature expansions. *Nucl. Phys.*, B582:277–295, 2000.

[88] M. Laine, M. Meyer, and G. Nardini. Thermal phase transition with full 2-loop effective potential. *Nucl. Phys.*, B920:565–600, 2017.